

Photo: Gustaaf Hallegraeff

## Chapter 4

### Vulnerability of open ocean food webs in the tropical Pacific to climate change

Robert Le Borgne, Valérie Allain, Shane P Griffiths, Richard J Matear,  
A David McKinnon, Anthony J Richardson and Jock W Young

*'The immense size of the Pacific is reflected in strong longitudinal differences in mixed layer depth and other physical circulation features, themselves reflected in the regional phytoplankton ecology.'* (Longhurst 2006)<sup>i</sup>

i Longhurst AR (2006) *Ecological Geography of the Sea*. Academic Press, New York, United States of America.

| <b>Contents</b>  | <b>Page</b> |
|--|-------------|
| <b>4.1 Introduction</b>  | <b>191</b>  |
| <b>4.2 General structure and function of food webs for tuna</b>                | <b>194</b>  |
| <b>4.3 Physical nature of the provinces in the region</b>                      | <b>201</b>  |
| 4.3.1 Pacific Equatorial Divergence  | 203         |
| 4.3.2 Western Pacific Warm Pool  | 204         |
| 4.3.3 North Pacific Tropical Gyre and South Pacific Subtropical Gyre           | 206         |
| 4.3.4 Archipelagic Deep Basins   | 206         |
| <b>4.4 Structure and variability of food webs in each province</b>             | <b>206</b>  |
| 4.4.1 Pacific Equatorial Divergence  | 206         |
| 4.4.2 Western Pacific Warm Pool  | 208         |
| 4.4.3 North Pacific Tropical Gyre and South Pacific Subtropical Gyre           | 210         |
| 4.4.4 Archipelagic Deep Basins   | 210         |
| 4.4.5 Overview of differences in food webs among provinces                     | 212         |
| <b>4.5 Critical requirements for maintenance of food webs in each province</b> | <b>214</b>  |
| 4.5.1 Macronutrients and micronutrients  | 214         |
| 4.5.2 Temperature  | 215         |
| 4.5.3 Dissolved oxygen   | 216         |
| 4.5.4 Solar radiation  | 216         |
| 4.5.5 Carbon dioxide   | 216         |
| <b>4.6 Recent observed changes in the food webs of provinces</b>               | <b>217</b>  |
| <b>4.7 Projected changes to the environment and food webs of provinces</b>     | <b>218</b>  |
| <b>4.8 Projected vulnerability of food webs in provinces</b>                   | <b>222</b>  |
| 4.8.1 Water temperature  | 222         |
| 4.8.2 Mixed layer depth  | 225         |
| 4.8.3 Upwelling  | 226         |
| 4.8.4 Solar and ultraviolet radiation  | 227         |
| 4.8.5 Dissolved oxygen   | 229         |
| 4.8.6 Ocean acidification  | 230         |
| <b>4.9 Integrated vulnerability assessment</b>                                 | <b>232</b>  |
| 4.9.1 Integrated assessments for each province                                 | 232         |
| 4.9.2 Ecopath model for the Warm Pool  | 235         |
| <b>4.10 Uncertainty, gaps in knowledge and future research</b>                 | <b>239</b>  |
| <b>4.11 Management implications and recommendations</b>                        | <b>241</b>  |
| <b>References</b>  | <b>242</b>  |

## 4.1 Introduction

The open sea areas of the tropical Pacific Ocean represent a vast area of fish habitat<sup>1</sup>. This expanse of ocean dwarfs the land in the region and makes up 98% of the total area under the jurisdiction of all Pacific Island countries and territories (PICTs) (Chapter 1).

Although much of this open ocean domain is relatively unproductive, it supports some of the largest tuna fisheries in the world. The total recent catches of skipjack tuna, yellowfin tuna, bigeye tuna and South Pacific albacore from the Western and Central Pacific Ocean (WCPO) is approximately 2.5 million tonnes per year, representing > 25% of the total global tuna catch (Chapters 1, 8 and 12).

The production of the four species of tuna, and other large pelagic fish, is underpinned by food webs based not only on the photosynthetic productivity of phytoplankton (called primary production) in the sunlit surface layer (photic zone) of the ocean, but also by bacteria and detritus, derived from phytoplankton. Most of this primary production occurs where nutrients, such as nitrogen, phosphorus and silicon, are transported to surface waters from the deeper layers of the ocean by the physical processes described in Chapter 3.

The energy produced through primary production moves through a 'trophic pyramid' via a range of zooplankton (such as copepods and larval fish), macrozooplankton (including jellyfish and salps) and micronekton (such as squid, shrimp and small fish), to sustain tuna and other large pelagic fish (Figure 4.1). The transfer of energy between each level in the trophic pyramid is generally only about 10% because (1) there are energy losses through respiration and excretion at each stage, and (2) the consumers in the next trophic level do not assimilate all available organic matter<sup>2</sup>. The various levels of the food web also contribute to the oceanic carbon sink by transferring carbon from the upper layers to the ocean depths through sinking of dead particles and the capture of prey from the photic zone by vertically migrating zooplankton and micronekton. This process, referred to as the 'biological carbon pump', helps reduce the concentrations of carbon dioxide (CO<sub>2</sub>) in the atmosphere<sup>3,4</sup>.

The availability of the nutrients that underpin the food web for tuna, together with suitable water temperatures and dissolved oxygen levels, determine the distribution and abundance of tuna and other large oceanic fish across the WCPO<sup>5,6</sup> (Chapter 8). Therefore, the responses of phytoplankton, zooplankton and micronekton to changes in the ocean processes that deliver nutrients to the photic zone, and to changes in the physical and chemical properties of the ocean projected to occur as a result of global warming and ocean acidification (Chapter 3), are expected to affect all life history stages of large oceanic fish.

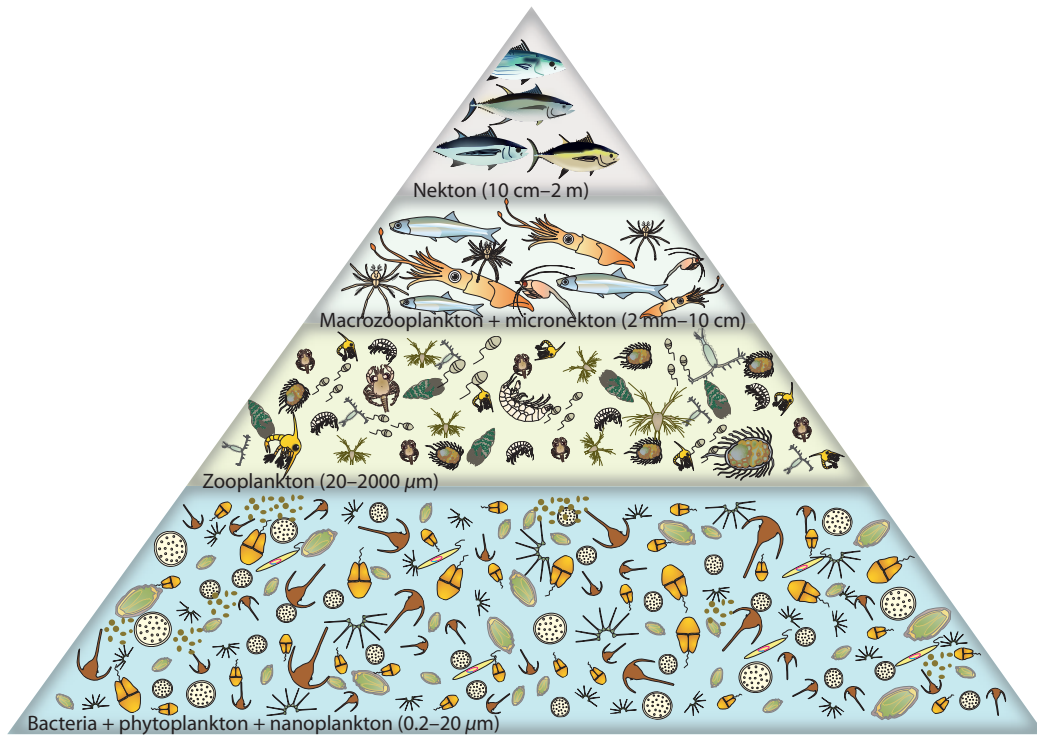


**Figure 4.1** Generalised trophic pyramid for the tropical Pacific Ocean. The base of the food web consists of bacteria, small phytoplankton and protists (nanozooplankton), 0.2–20  $\mu\text{m}$  in size. These organisms are ingested by zooplankton, such as crustaceans, molluscs or tuna larvae, up to a size of 2000  $\mu\text{m}$ . In turn, zooplankton are consumed by macrozooplankton, such as jellyfish, and micronekton, such as squid, shrimp and small fish. Micronekton and, to a lesser extent, macrozooplankton are the prey for tuna and other large pelagic fish at the top of the pyramid (see Table 4.1 for size ranges).

The purpose of this chapter is to (1) summarise what is known about the structure of the food webs that underpin the production of tuna across the region and describe how these food webs have changed recently; and (2) project how these food webs are likely to change by 2035 and 2100 under low (B1) and high (A2) emissions scenarios defined by the Intergovernmental Panel on Climate Change (IPCC) and outlined in Chapter 1. In making these assessments, we recognise that we are dealing with a vast part of the tropical Pacific Ocean, and that there is considerable variation in the nature of the food webs that support tuna across this region. To explain and examine this variation, we have arranged this chapter around the well-recognised ecological provinces of the region<sup>1</sup>.

To set the scene, we summarise the structure and function of oceanic food webs in general, the physical nature of the ecological provinces in the region, the differences in food webs among these provinces, and the environmental conditions needed to maintain them. We then progress to describing the recent observed changes in the physical nature of the provinces and their food webs, and the projected vulnerability

of food webs in each province to climate change. To assess this vulnerability, we have applied the framework outlined in Chapter 1 and used the projected changes to availability of nutrients, water temperature, mixed layer depth, upwellings, solar and ultraviolet radiation, dissolved oxygen and acidification of the ocean described in Chapter 3 to assess the exposure of phytoplankton, zooplankton and micronekton to global warming and increased emissions of CO<sub>2</sub>. We have also used an NPZ (Nutrient-Phytoplankton-Zooplankton) model linked to a global climate model<sup>7</sup> (the IPSL-CM4-IPSL-LOOP coupled-climate carbon model) to integrate the projected changes to the physical and chemical features of the tropical Pacific Ocean and estimate changes in net primary production (NPP) and biomass of zooplankton in all provinces. For one province, the Warm Pool in the western Pacific, we then use projected changes in primary production in an Ecopath model to estimate the effects on zooplankton, micronekton and tuna.

**Table 4.1** The sources of food that build the food web for tuna and other large pelagic fish in the tropical Pacific Ocean, together with their size, representative organisms, trophic status and depth of their habitat. The first three sources of food belong to the ‘paraprimary’ level, which is at the base of the food web, like primary production, but is not the direct result of photosynthesis (source: Legand et al. 1972, Dussart 1965, UNESCO 1968)<sup>22,131,132</sup>.

| Food source              | Size range             | Representative organisms   | Trophic status           | Depth of habitat |
|--------------------------|------------------------|--|--------------------------|------------------|
| Dissolved organic matter | < 0.2 $\mu\text{m}$    |  | Paraprimary level        | All depths       |
| Detritus                 | > 0.2 $\mu\text{m}$    |  | Paraprimary level        | All depths       |
| Heterobacteria           | > 0.2 $\mu\text{m}$    |  | Paraprimary level        | All depths       |
| Picophytoplankton        | 0.2–2 $\mu\text{m}$    | Cyanobacteria ( <i>Prochlorococcus</i> , <i>Synechococcus</i> ), pico-eukaryotes | Primary level            | Photic zone      |
| Nanophytoplankton        | 2–20 $\mu\text{m}$     | Diatoms, dinoflagellates, haptophytes, pelagophytes                              | Primary level            | Photic zone      |
| Microphytoplankton       | 20–200 $\mu\text{m}$   | Diatoms, dinoflagellates, filamentous cyanobacteria ( <i>Trichodesmium</i> )     | Primary level            | Photic zone      |
| Nanozooplankton          | 2–20 $\mu\text{m}$     | Heterotrophic flagellates, small ciliates  | Secondary level          | All depths       |
| Microzooplankton         | 20–200 $\mu\text{m}$   | Radiolarians, foraminiferans, tintinnids, larval copepods                        | Secondary level          | All depths       |
| Mesozooplankton          | 200–2000 $\mu\text{m}$ | Copepods, chaetognaths, larvaceans, ostracods, doliolids, larval fish            | Secondary/tertiary level | All depths       |
| Macrozooplankton         | 2–20 mm                | Pteropods, heteropods, siphonophores, jellyfish, salps                           | Secondary level and over | All depths       |
| Epipelagic micronekton   | 2–10 cm                | Small fish, amphipods, cephalopods, and shrimp                                   | Secondary level and over | 0–200 m          |
| Mesopelagic micronekton  | 2–10 cm                | Small fish, amphipods, cephalopods, and shrimp                                   | Secondary level and over | 200–500 m        |
| Deep micronekton         | 2–10 cm                | Fish, cephalopods, and shrimp  | Secondary level and over | > 500 m          |

We conclude by reviewing the uncertainty of these projections, identifying gaps in knowledge and priorities for future research, and recommending a few management measures that could potentially help reduce the vulnerability of the food webs vital to tuna. We emphasise that adaptation options alone may not be sufficient, and that avoiding dangerous outcomes for oceanic food webs will also depend on reducing greenhouse gas emissions worldwide<sup>8</sup>.

## 4.2 General structure and function of food webs for tuna

### 4.2.1 Phytoplankton production: regenerated and new

All production of phytoplankton at the base of food webs for tuna and other large pelagic fish occurs in the photic zone, where there is sufficient light for photosynthesis (Figure 4.2). This primary production uses nutrients regenerated within the photic zone and 'new' nutrients transferred there from deeper water by the processes described in Chapter 3 (Box 4.1). Regenerated nutrients, consisting mainly of ammonium ( $\text{NH}_4$ ) and soluble reactive phosphorus (SRP), lead to 'regenerated production', whereas the nutrients involved in 'new production' are nitrates ( $\text{NO}_3$ ) and di-nitrogen ( $\text{N}_2$ ), SRP and silicates. Availability of nitrogen, in the form of either ammonium or nitrate, is the main factor limiting the primary productivity in most oceanic ecosystems, although the supply of SRP or micronutrients such as iron (Fe) can also limit production. Regenerated nutrients alone are not sufficient to support primary production – a minimum level of new nutrients is needed to compensate for losses that occur within the photic zone, and to maintain the production of phytoplankton.

The vertical structure of the water column determines the availability of new nutrients in the photic zone and four different situations are found in the tropical Pacific (Figure 4.3). In regions where there is a pronounced thermocline (Cases 1 and 2), transfer of nutrients to the mixed layer is inhibited because the thermocline acts as a barrier to exchanges between nutrient-rich deep layers and the superficial mixed layer. In such situations, when the thermocline is deep (Case 1), new production is low because it occurs only in the lower part of the photic zone with low light intensity. In Case 1, NPP which is the sum of new and regenerated production, is low. In situations where the thermocline is shallower (Case 2), NPP is higher due to more new production occurring in the nutrient-rich water of the photic zone, below the thermocline. In other words, the deeper the thermocline, the lower the new production and NPP<sup>9</sup>.

In regions where the thermocline is weak, exchanges between the deep nutrient-rich layers and the photic zone are easier than in Cases 1 and 2. These exchanges occur through processes like turbulence, mixing, and diffusion, which then drive new production. In the gyres in the northern and southern tropical Pacific, however, the anticyclonic circulation, with prevailing downwelling conditions, leads to a

very deep and weak thermocline. In this case, physical nutrient supply is inefficient at transporting nutrients into the photic zone (Case 3), except via temporary eddies linked to wind bursts. Consequently, production in the photic zone of these gyres is very low.

Finally, where there is strong upwelling (vertical transport of deeper water masses to the surface), new nutrients are brought into the whole photic zone, leading to high new production (Case 4).

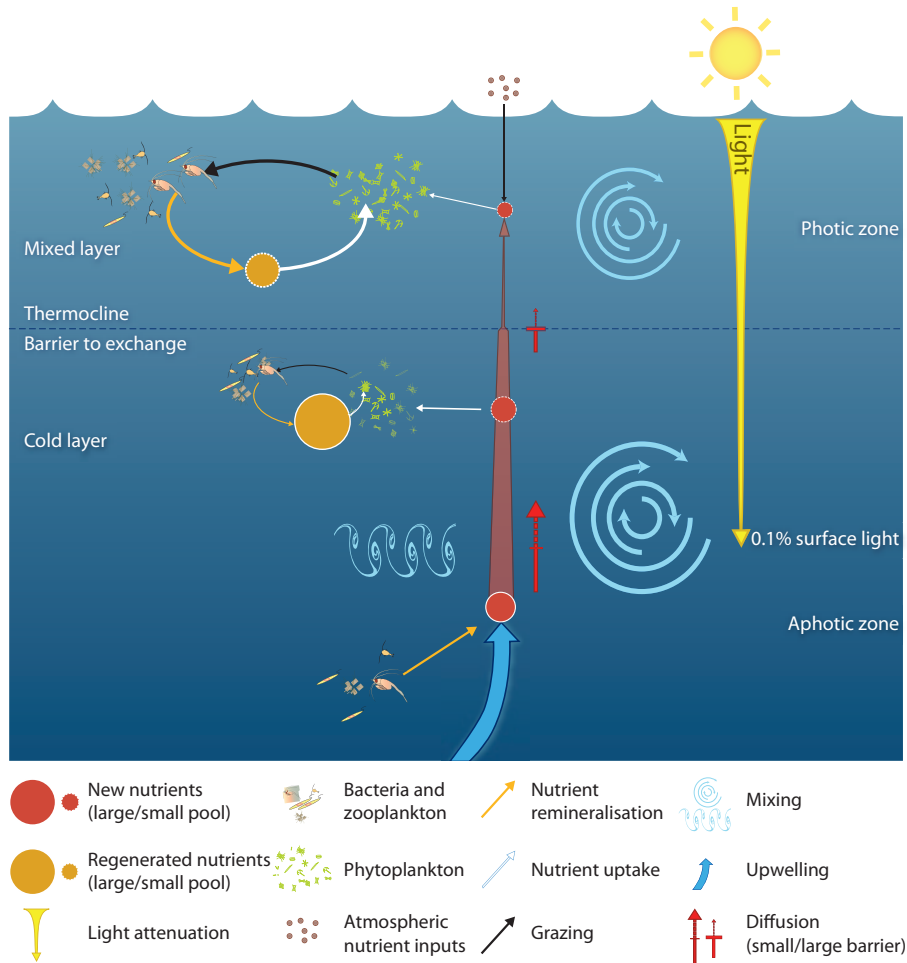
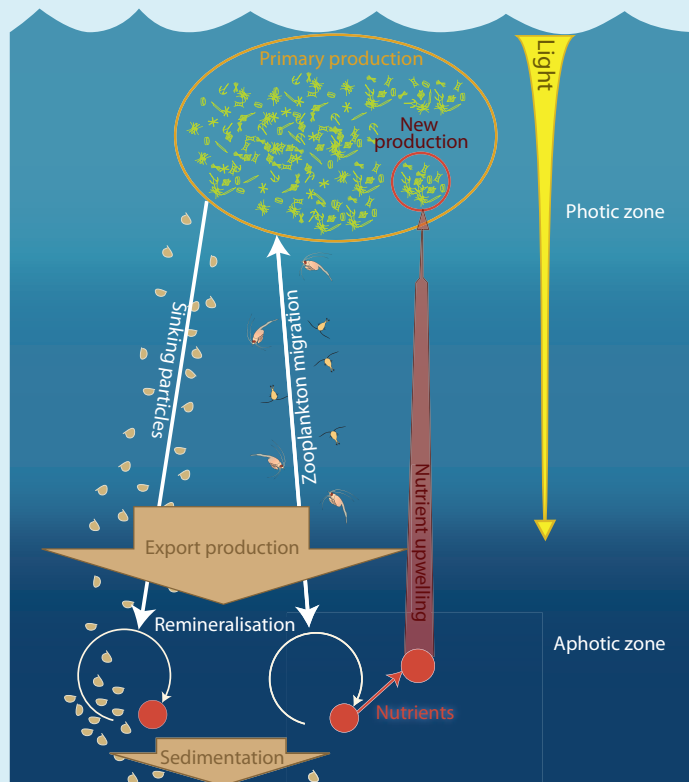


**Figure 4.2** Key features of the surface layer of the ocean that determine primary production. The photic zone, where photosynthesis occurs, typically extends to the depth that receives 0.1% of the surface light intensity in tropical areas. Below this, is the aphotic zone, where there is insufficient light for photosynthesis. The warmer mixed surface layer is separated from the deeper cold layer at the thermocline, where water temperature decreases abruptly. The thermocline is a barrier to mixing and the transfer of nutrients from cold, deep water to the surface mixed layer. The cold layer is supplied with nutrients brought up from the aphotic zone by mixing, diffusion and vertical advection (upwelling), depending on the location.

### Box 4.1 Primary and export production in the ocean

Primary production is the generation of organic matter in the photic zone by photosynthetic phytoplankton. Primary production is based on two types of nutrients (1) regenerated nutrients released from decaying phytoplankton and zooplankton after they die, and from the respiration and excretion of zooplankton; and (2) 'new' nutrients originating outside the photic zone and delivered there through physical processes such as upwelling, mixing and diffusion.

Export production is the amount of organic matter that leaves the photic zone, typically through sinking of dead plant and animal particles, including faecal pellets, towards the deeper layers of the ocean. Much of the exported organic matter is remineralised by bacteria and zooplankton below the photic zone to produce new nutrients. Part of the export production reaches the sediments at the bottom of the ocean. In balanced ('steady state') ecosystems, the biomass of plankton is fairly constant over the short term, which implies that losses are balanced by inputs to the system. Thus, in the photic zone, export production is balanced by new production, that is, nutrients produced in the deeper layers through mineralisation are brought to the photic layer, converted into organic matter by photosynthesis, and exported.



The source of nutrients also influences the composition of the phytoplankton. New primary production is usually dominated by diatoms because they out-grow other phytoplankton<sup>10</sup>. However, diatoms are replaced by other phytoplankton (e.g. haptophytes and pelagophytes) where the supply of silicon limits growth because diatoms cannot construct their shells without it<sup>11</sup>. In turn, the size composition of the phytoplankton determines the type and size of zooplankton that graze them. Relatively large zooplankton grazers (mesozooplankton), like copepods (Table 4.1), dominate areas of new primary production, feeding on the diatoms and large phytoplankton common there. On the other hand, regenerated primary production is dominated by tiny phytoplankton (picophytoplankton) (Table 4.1), which are grazed by very small zooplankton (nanozooplankton), such as heterotrophic flagellates and ciliates<sup>12</sup> (Table 4.1). In general, therefore, food webs supporting tuna based on significant new production and larger phytoplankton tend to have fewer trophic levels.

New production is augmented by the uptake of  $N_2$ , a dissolved gas, in a process called 'diazotrophy'. The main organisms supported by  $N_2$  (diazotrophs) are unicellular cyanobacteria<sup>13</sup>, endosymbiots (e.g. *Richelia* sp.) and filamentous cyanobacteria, particularly those of the genus *Trichodesmium* which bloom in summer<sup>14</sup>. Large populations of cyanobacteria can help alleviate the effects of nitrogen limitation in oligotrophic regions, where they can contribute 30–50% of new production<sup>15</sup>. However, the contribution of blooms of cyanobacteria to the food web appears to be highly variable, and is still controversial.

Abundances of zooplankton have also sometimes been linked to blooms of *Trichodesmium*<sup>16</sup>. However, a high biomass of cyanobacteria does not always result in increased productivity of zooplankton because some cyanobacteria are toxic or unpalatable, except to harpacticoid copepods<sup>17</sup>. In such situations, the decayed organic matter from cyanobacteria needs to be mineralised before contributing to a new production cycle that may support other grazers.

#### 4.2.2 Other parts of the food web (bacteria, zooplankton and micronekton)

Whereas primary production by phytoplankton is based on the uptake of inorganic compounds, all other parts of the food web rely on ingesting organic matter, a process known as 'heterotrophy'. This organic matter is consumed in solution by bacteria, but is in the form of 'particles' when consumed by zooplankton and micronekton (Table 4.1). The biomass of 'heterotrophic' organisms depends on the amount of organic matter produced by phytoplankton, either as dissolved compounds released by excretion or in a particulate form resulting from NPP. In general terms, therefore, the abundance and diversity of species in the food web of open ocean ecosystems relies primarily on the level of phytoplankton production.

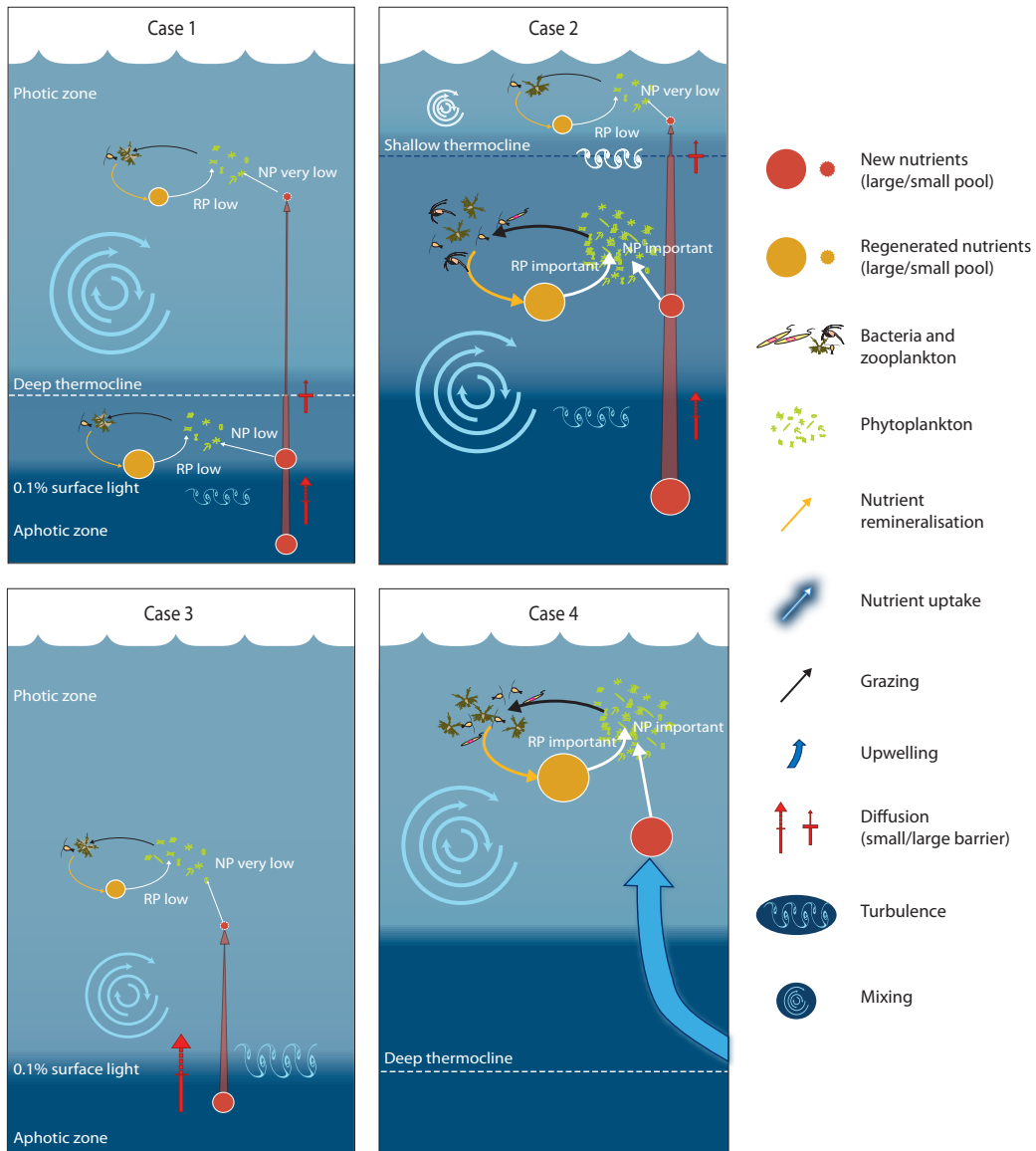


**Figure 4.3** Four typical cases of variation in vertical hydrographic structure and its effect on production of phytoplankton in the tropical Pacific Ocean. In Case 1, the thermocline is deep but still in the photic zone; primary production based on regenerated nutrients dominates in the mixed layer but is supplemented by some new production (NP) below the thermocline. In Case 2, the mixed layer remains nutrient-poor (oligotrophic) but a shoaling of the thermocline allows cold, nutrient-rich water to increase both regenerated production (RP) and NP substantially within the photic zone below the thermocline. In Case 3, the thermocline is weak and deep, allowing some inputs of 'new' nutrients from the deep oligotrophic waters to enter the photic zone. However, the biomass of phytoplankton is low and driven mainly by RP. In Case 4, new nutrients delivered by upwelling supply the entire photic zone, even though the thermocline is deep, permitting significant NP and high RP. Note that the photic zone is shallower in Cases 2 and 4 because the higher concentrations of plankton there reduce light penetration.

However, observations have shown that production of small phytoplankton and bacteria are similar and that the production of phytoplankton is supplemented by production based on the contributions of heterotrophic bacteria and detritus (non-living particles) (Table 4.1). This resulted in the concept of the ‘microbial loop’<sup>18</sup>, which was originally pictured as a parallel model of trophic structure to the classical food web<sup>19</sup>. It is now recognised that the classical and microbial food webs are linked through processes of coagulation and the formation of ‘marine snow’, i.e. particles rich in microbes available to mesozooplankton grazers<sup>20</sup> (Figure 4.4).

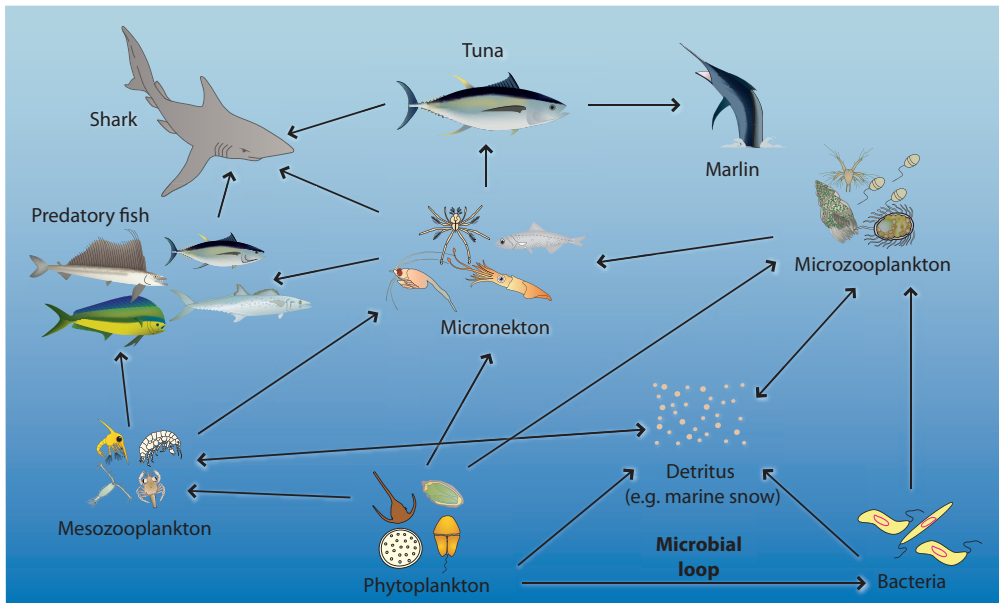


**Figure 4.4** Generalised food web supporting tuna and other large pelagic fish. Note that in the lower levels of the food web, the classical and microbial pathways are linked through formation of ‘marine snow’ and other detritus.

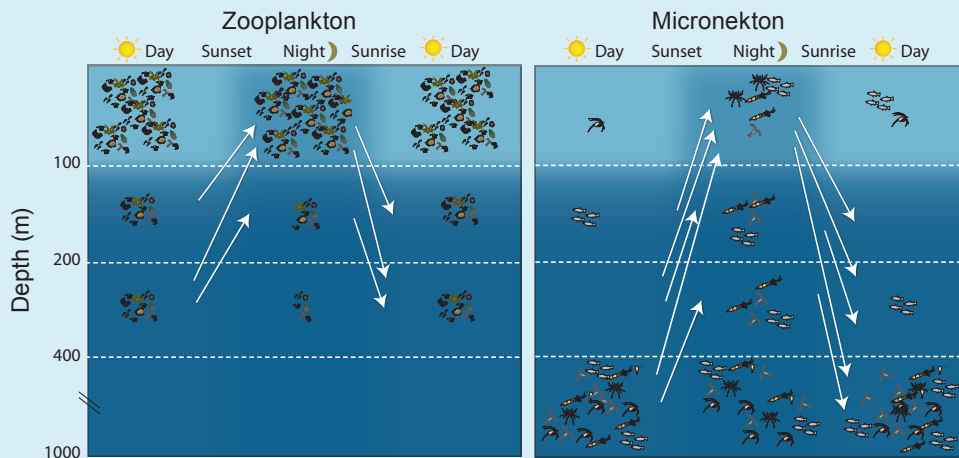
The zooplankton that graze on phytoplankton and ‘marine snow’, and the micronekton that consume zooplankton, are not distributed evenly in the water column. The main factors that determine their distribution are their swimming ability and the location of the nutrients supporting the phytoplankton on which they depend. Zooplankton and micronekton migrate towards the surface at dusk and to deeper water at dawn in search of food, and to avoid predators (Box 4.2). This results in different biomasses of zooplankton and micronekton within the water column during the day and night. The larger the organisms, the greater the migrations, so that diel variations in abundance of micronekton in the photic zone are greater than those of the zooplankton<sup>21</sup>.

There is also a relationship between the minimum depth of the nutrient-rich water below the surface, i.e. the ‘nutricline’ associated with the thermocline (Chapter 3), and phytoplankton production and mesozooplankton biomass. For example, in the

### Box 4.2 Vertical migrations of zooplankton and micronekton

Many zooplankton and micronekton migrate from deeper parts of the water column to the surface at sunset, and return at sunrise. Micronekton move to surface waters from depths of up to 1000 m, whereas zooplankton generally migrate from waters < 400 m deep (see figure below). In addition, some phytoplankton, such as dinoflagellates, make small migrations within the photic zone linked to light intensity. However, not all zooplankton and micronekton migrate as far as the photic zone at night – many species only reach the upper levels of the aphotic zone. Other zooplankton and micronekton do not migrate at all, or do so only on a small scale. These organisms are known as ‘non-migrants’ and their biomass can only be estimated at night, once the migrants have departed.

Both zooplankton and micronekton migrate at night to feed. The migrating zooplankton prey on phytoplankton and tiny organisms (e.g. bacteria attached to detritus and microzooplankton), which inhabit the photic zone. Micronekton migrate to feed on zooplankton living permanently in the upper layers of the water column, and those that move there at night. The migrating zooplankton and micronekton leave the photic zone at sunrise to avoid predators and seek shelter in the dim waters of the aphotic zone.



The intensity of vertical migrations to the photic zone by zooplankton is linked to the abundance of phytoplankton. Little migration of mesozooplankton (200–2000  $\mu\text{m}$  in size) occurs in areas of the ocean rich in nutrients because mesozooplankton remain closely linked to phytoplankton and the associated small organisms in the photic zone during day and night. In oligotrophic areas, however, mesozooplankton are not tightly linked to phytoplankton and have a more diverse feeding regime. This results in marked differences in the night/day ratio of mesozooplankton biomass within the photic zone between nutrient-rich and nutrient-poor areas. When the nutricline is deep and net primary production (NPP) is low, the mesozooplankton night/day ratio is higher than where the nutricline is shallower (Figure 4.5d). The effect of changes in NPP on the intensity of vertical migrations by micronekton is still unknown.

tropical western Pacific (Figure 4.5), both the production of phytoplankton and the biomass of mesozooplankton increase as the depth of the nutricline decreases (Figure 4.5). The proportion of mesozooplankton occurring within the first 100 m of the water column also increases as nutricline depth decreases because there is greater new primary production when the nutricline is shallow. In addition, the depth of the nutricline also affects the diel vertical migrations of mesozooplankton (Figure 4.5). When the nutricline is deep, causing more oligotrophic conditions in surface waters, the vertical night-time movements of mesozooplankton increase, indicating that coupling between mesozooplankton and surface phytoplankton biomass is reduced in such places. Finally, the percentage contribution of small zooplankton (microzooplankton) is greater in oligotrophic areas, where the nutricline is deep. The opposite is true for the larger mesozooplankton (500–2000  $\mu\text{m}$ ) (Figure 4.5).

The deep and dark ocean below the photic zone follows different rules. Deep currents may have different directions to those at the surface, and vertical hydrological gradients are generally weaker, making exchanges easier between water masses. Nevertheless, as indicated earlier, the photic zone and deep ocean ecosystems are inter-related – organisms living at depth need to get their energy from the photic layer by vertical migrations, or by heterotrophic processes based on sinking particles, or from other organisms of the deep ocean. Even so, non-migrating species living below the photic zone at all times represent more than half of the micronekton biomass<sup>22</sup>.

The most important part of oceanic food webs from a fisheries perspective – the link between micronekton and tuna – is still quite poorly understood. Several studies on the feeding ecology of tuna<sup>21,23–26</sup> have shown that their diets consist mainly of small fish, squid and crustaceans. The proportions of these three categories of micronekton vary within and between tuna species, and among life history stages, regions, time of the year and the depth preferences of the fish<sup>25,27–29</sup>. A full understanding of potential changes in the micronekton prey of tuna will eventually involve more specific knowledge of tuna dietary requirements at different stages of development, and for reproduction.

### 4.3 Physical nature of the provinces in the region

Five ecological provinces cover the area of the tropical Pacific Ocean that is the focus of this book<sup>1</sup>. These provinces are the Pacific Equatorial Divergence, Western Pacific Warm Pool, North Pacific Tropical Gyre, South Pacific Subtropical Gyre and Archipelagic Deep Basins (Figure 4.6). The borders of these provinces are generally defined by convergence zones of surface currents, and each province has a specific wind regime and vertical hydrological structure. Note that a simplified definition of the borders of provinces has been used for the modelling described in Section 4.7.

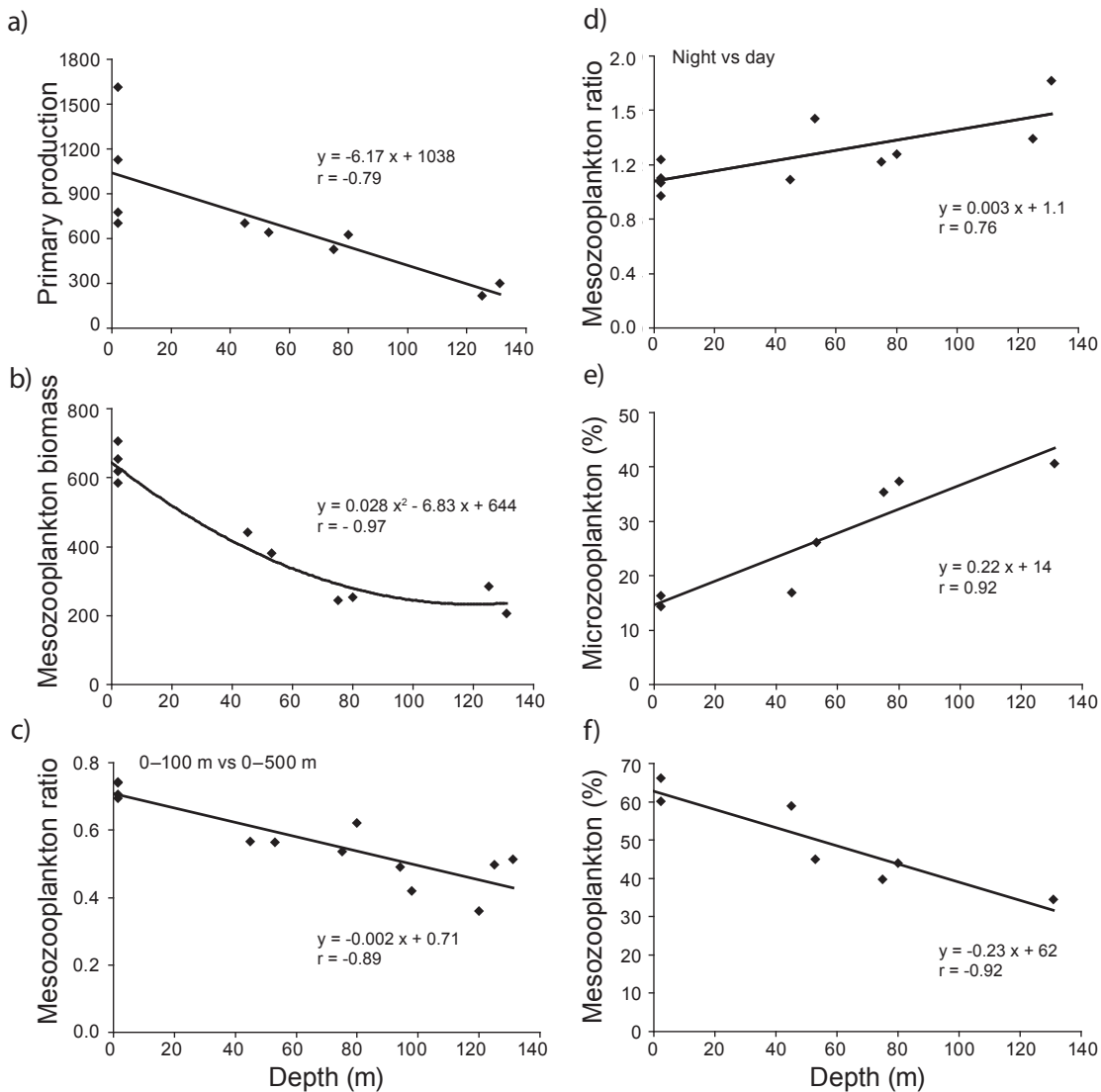


**Figure 4.5** Relationships between the minimum depth of the nutricline (defined as  $\text{NO}_3 = 0.1 \mu\text{M}$ ) and (a) primary production (mg C per m<sup>2</sup> per day); (b) mesozooplankton biomass (0–200 m, mg C per m<sup>2</sup>); (c) vertical distribution of mesozooplankton (0–100 m: 0–500 m ratio); (d) diel variation in biomass of mesozooplankton within the upper 200 m of the water column (night:day ratio); (e) microzooplankton (35–200  $\mu\text{m}$ ) as a percentage of total zooplankton biomass; and (f) large mesozooplankton (500–2000  $\mu\text{m}$ ) as a percentage of total zooplankton biomass, in the tropical western Pacific Ocean. Data are from 7-day-long time-series stations in the tropical Pacific (source: Institut de Recherche pour le Développement)<sup>75</sup>.

The locations of the Pacific Equatorial Divergence and the Western Pacific Warm Pool can also change dramatically from year to year, depending on the prevailing El Niño-Southern Oscillation (ENSO) conditions, which alters the extent of upwelling in the eastern and central equatorial Pacific and the nitrate concentrations of the surface waters<sup>30</sup>. The Archipelagic Deep Basins Province, as the name implies, is characterised by the occurrence of many archipelagos and seamounts. It is a

patchwork of processes, on a variety of spatial scales, with varied vertical structures, driven by the way the landmasses divert surface currents and create eddies (Chapter 3). This province also receives nutrients due to runoff from the high islands located there.

As outlined in Section 4.2.1 and Figure 4.3, the vertical hydrological structure and associated physical processes of each province have a profound effect on the phytoplankton productivity available to supply the base of the food web. In particular, the features of each province mediate access to the new nutrients needed for primary production. Although regenerated nutrients also contribute to the growth of phytoplankton, the amount of new production is determined by inputs of nutrients from deep water to the photic zone and varies among provinces, in line with the well known correlation between primary production and the depth of the nutricline<sup>9</sup> (Figure 4.5).

The main characteristics of the five provinces are described below, based on the features of atmospheric climate in the region and the tropical Pacific Ocean described in Chapters 2 and 3.

### 4.3.1 Pacific Equatorial Divergence

The Pacific Equatorial Divergence (PEQD) is generated by the effects of the earth's rotation (Coriolis force) on the South Equatorial Current (SEC) in the two hemispheres (Chapter 3). As a result of this divergence, there is significant upwelling of new nutrients from below the photic zone (Case 4, Figure 4.3), creating the richest surface waters in the tropical Pacific. The waters of PEQD are characterised by higher salinity, partial pressure of CO<sub>2</sub> (pCO<sub>2</sub>), nutrient concentrations and phytoplankton abundance (chlorophyll *a*) (Figure 4.7). These nutrient-rich waters span much of the equatorial Pacific and drift polewards before submerging at the convergence with the North Equatorial Counter Current (NECC) (ca. 5°N) and the South Equatorial Counter Current (SECC) (ca. 6°S–8°S) (Figure 4.8). At these convergences, particulate organic matter sinks and is remineralised, leading to low levels of dissolved oxygen (see Chapter 3 for more details).

Ironically, although the macronutrients (nitrate, SRP and silicate) available in PEQD exceed those needed for prolific growth of phytoplankton, primary production in this province is limited by low concentrations of iron (Figure 4.9). The iron in PEQD is derived from Papua New Guinea (PNG) and is delivered by the eastward-flowing New Guinea Coastal Undercurrent<sup>31</sup>, and Equatorial Undercurrent (EUC), and possibly from thermal vents and atmospheric dust. However, the quantities are insufficient to enable all the macronutrients in PEQD to be used by phytoplankton. Consequently, PEQD acts like a buffer: regardless of the level of macronutrients, phytoplankton biomass remains relatively constant because the large reservoir of nutrients enables primary productivity to continue for several months if nutrient inputs are temporarily reduced for climate-related reasons<sup>30</sup>. This occurred during the strong 1982–1983 and 1997–1998 El Niño events<sup>30,32</sup>.

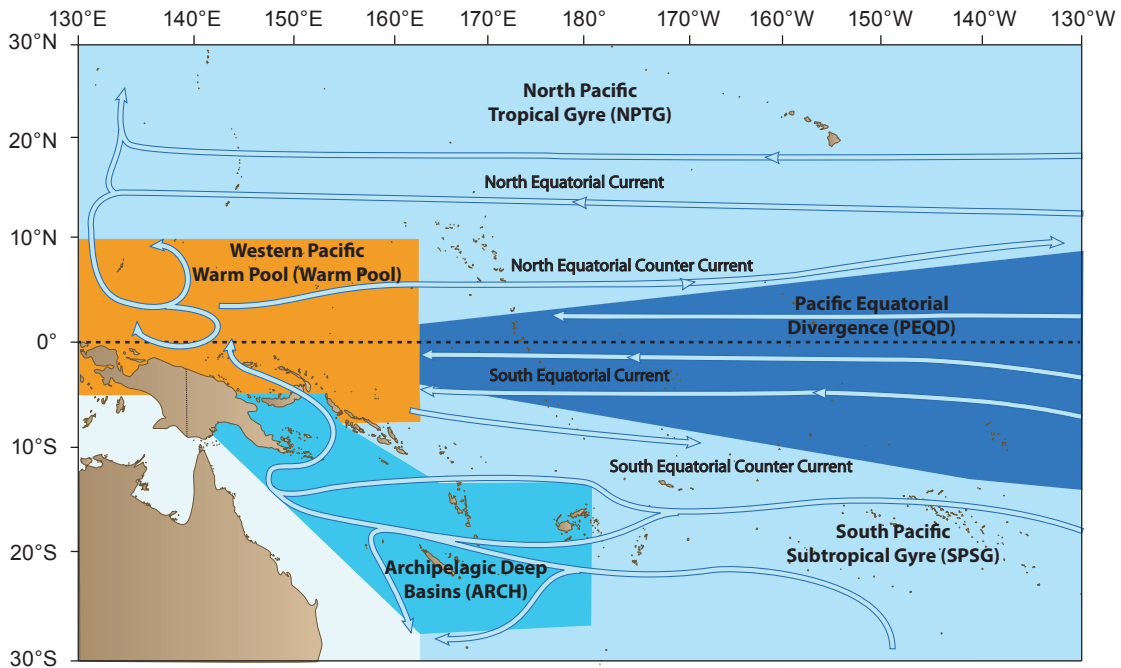


**Figure 4.6** The five ecological provinces of the tropical Pacific Ocean defined by Longhurst (2006)<sup>1</sup>, together with the major ocean currents of the region.

The surface waters of PEQD also drift to the west until they converge with the Western Pacific Warm Pool (see below) (Figure 4.8). The border between PEQD and the Warm Pool is marked by a clear ‘front’ in salinity,  $p\text{CO}_2$ , chlorophyll *a* and zooplankton<sup>33</sup>. The convergence zone between PEQD and the Warm Pool changes due to variation in the strength and longitudinal extension of the SEC between seasons and among years, in response to ENSO events (Chapter 3). During strong La Niña episodes, the front reaches the far western side of the equatorial Pacific, causing a great reduction in the size of the Warm Pool. During El Niño events, the front moves to the east and may reach the Galapagos Islands, causing PEQD to disappear<sup>32</sup>. Such fluctuations of the surface area of PEQD and the Warm Pool can be seen by ocean colour imagery<sup>34</sup> and predicted from climatic indices, such as the Southern Oscillation Index (SOI)<sup>35</sup>. From 1980 to 2000, the mean longitude of the border between PEQD and the Warm Pool was 178°W<sup>30</sup>, almost on the dateline.

### 4.3.2 Western Pacific Warm Pool

In contrast to PEQD, the surface waters of the Western Pacific Warm Pool (Warm Pool) have a significantly lower salinity due to high rainfall (Chapter 2), and are nutrient-depleted because there is no upwelling in this province. The thermocline in the Warm Pool is relatively deep (~ 80 m) under average climatic conditions, being located close to the lower limit of the photic zone (Case 1, Figure 4.3). The thermocline

has a strong temperature gradient (Figure 4.7), which forms a considerable barrier to the transfer of nutrients to the surface layer. This situation changes markedly during El Niño episodes, when there is a shoaling of the thermocline to a depth of ~ 40 m (Case 2, Figure 4.3). When this occurs, there is an increase in primary production, stimulated by the supply of more new nutrients to the photic zone below the thermocline (Figures 4.7). Despite the fact that the Warm Pool is low in nutrients, the greatest catches of skipjack and yellowfin tuna are often made in this part of the region (see Section 4.4.2 and Chapter 8 for a possible explanation for this conundrum).

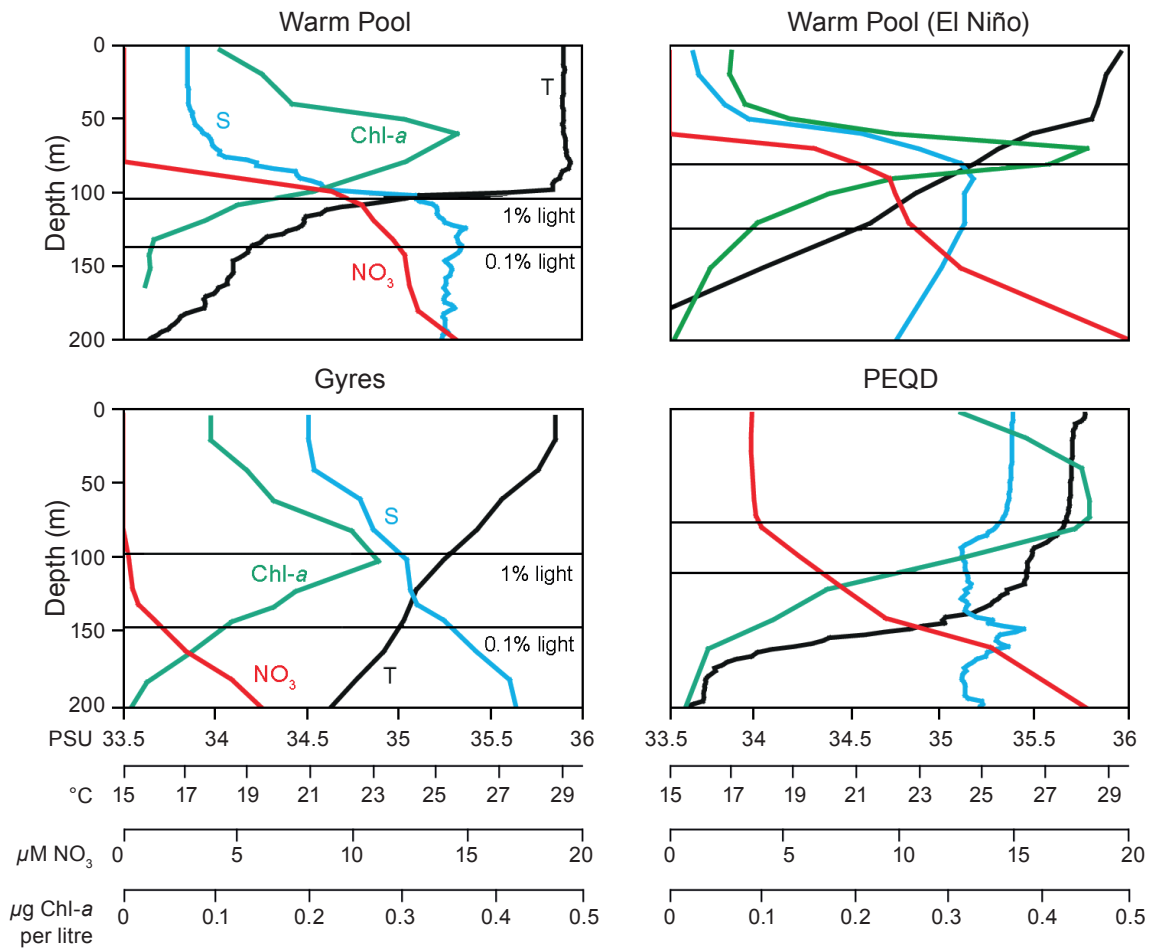


**Figure 4.7** Observed vertical profiles of temperature (T in °C), salinity (S in PSU), nitrate concentration (NO<sub>3</sub>) and chlorophyll *a* (Chl-*a*) to a depth of 200 m from different provinces to illustrate concepts shown on Figure 4.3. The Warm Pool corresponds to Case 1, the Warm Pool (El Niño) is Case 2, the two Gyres (NPTG and SPSG) are Case 3 and the Pacific Equatorial Divergence (PEQD) is Case 4 on Figure 4.3. Note the more or less steep thermal and salinity gradients between provinces, the associated levels of NO<sub>3</sub> and the depths of maximum chlorophyll *a*. Two different light levels, 1.0% and 0.1%, are presented to indicate the lower limits of the photic zone (source: Institut de Recherche pour le Développement)<sup>75</sup>.

### 4.3.3 North Pacific Tropical Gyre and South Pacific Subtropical Gyre

On both sides of the equatorial band, the large atmospheric anticyclones in the northern and southern subtropical Pacific generate oceanic gyres (Chapter 3). The provinces covered by these large gyres are known as the North Pacific Tropical Gyre (NPTG) (also known as the North Pacific Subtropical Gyre) and the South Pacific Subtropical Gyre (SPSG) (Figure 4.6). They are characterised by a very deep but weak thermocline (Figure 4.7), which allows some nutrient inputs to the photic zone from deep water through mixing and diffusion (Case 3, Figure 4.3). However, during summer, a strong and shallower (40–60 m) thermocline is superimposed on the main thermocline, due to the increase in solar radiation, creating a great barrier to nutrient inputs (Case 1, Figure 4.3). This leads to lower primary production in the upper part of the photic zone in summer compared with the rest of the year.

### 4.3.4 Archipelagic Deep Basins

The western part of SPSG is characterised by a large number of islands and shallow seamounts<sup>36</sup>, which alternate with oceanic basins. For this reason, it is referred to as the Archipelagic Deep Basins province (ARCH) (Figure 4.6). In this province, availability of nutrients from runoff can be significant in the vicinity of high islands. In addition, current regimes are more complex due to the way islands, archipelagos or seamounts divert oceanic circulation through a range of mesoscale processes (Chapter 3). These processes include upwelling or downwelling, cyclonic or anticyclonic eddies in the lee of the islands, frontal zones and an increase of amplitude in internal waves (Chapter 3). The result is that ARCH is a mosaic of surface waters with different characteristics, in contrast to the other provinces, which are generally dominated by more stable large-scale processes.

## 4.4 Structure and variability of food webs in each province

### 4.4.1 Pacific Equatorial Divergence

The biological features of the food web in PEQD are relatively stable along the equatorial band (1°N–1°S) from east to west<sup>30</sup>. However, marked variations occur in relation to the maturation of the ecosystem as waters from PEQD move polewards (Figure 4.8), with an increasing contribution of regenerated production to total phytoplankton production<sup>37</sup>. Nevertheless, the ratio between phytoplankton and heterotrophs (bacteria and zooplankton) remains relatively constant<sup>38</sup>, thus indicating steady state (or balanced) ecosystems.

Most of the food web in PEQD is concentrated in the upper 100 m of the water column because of the availability of high levels of nutrients within the photic zone (Figure 4.10a). Another important feature of this food web is the prominence at all

depths of ‘marine snow’ (particles  $> 500 \mu\text{m}$ ), studied only in this province<sup>39</sup>. While the nutritional value of marine snow is poorly understood, it may provide zooplankton with a significant source of particulate carbon<sup>39</sup>. Some of the relatively large marine snow particles are produced at the equator and drift to the convergence zone with the Warm Pool (Figure 4.8), where they sink and return to the equator due to deep circulation, via the ‘latitudinal conveyor belt’<sup>39</sup>. Transfer of phytoplankton and other particles also occurs between PEQD and the Warm Pool (Section 4.4.2).

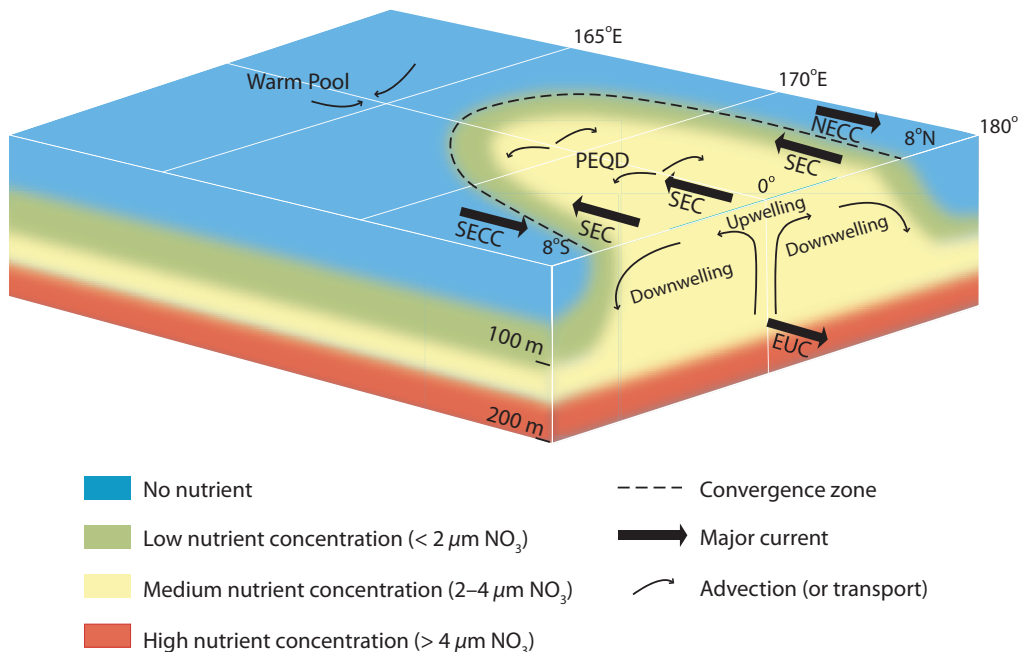


**Figure 4.8** Upwelling in Pacific Equatorial Divergence (PEQD) province. Nutrient-rich waters are brought to the surface from the Equatorial Undercurrent (EUC) and carried to the north and south by upwelling. Eventually, they plunge at the convergences between the South Equatorial Current (SEC) and South Equatorial Counter Current (SECC), and with the SEC and the North Equatorial Counter Current (NECC). The SEC also carries the upwelled waters to the west until they converge with the Warm Pool, at a salinity front, a region with distinct concentrations of dissolved carbon dioxide, nutrients and phytoplankton. Based on satellite images and data from the EBENE cruise along 180° in 1996 (source: Eldin and Rodier 2003)<sup>126</sup>.

The ecosystem within PEQD is relatively stable due to iron limitation (Section 4.3.1). As a result, interannual changes, as depicted by the SOI, affect the overall surface area of PEQD but not the structure of its ecosystem. For example, when the SOI is positive (La Niña), the PEQD ecosystem remains the same from the Galapagos Islands to its border with the Warm Pool, west of the dateline. However, tropical instability waves (TIWs) can cause temporary spatial rearrangements of hydrography and planktonic biomasses<sup>30</sup>, mainly east of the dateline and at the northern convergence between SEC and NECC (Figure 4.8).

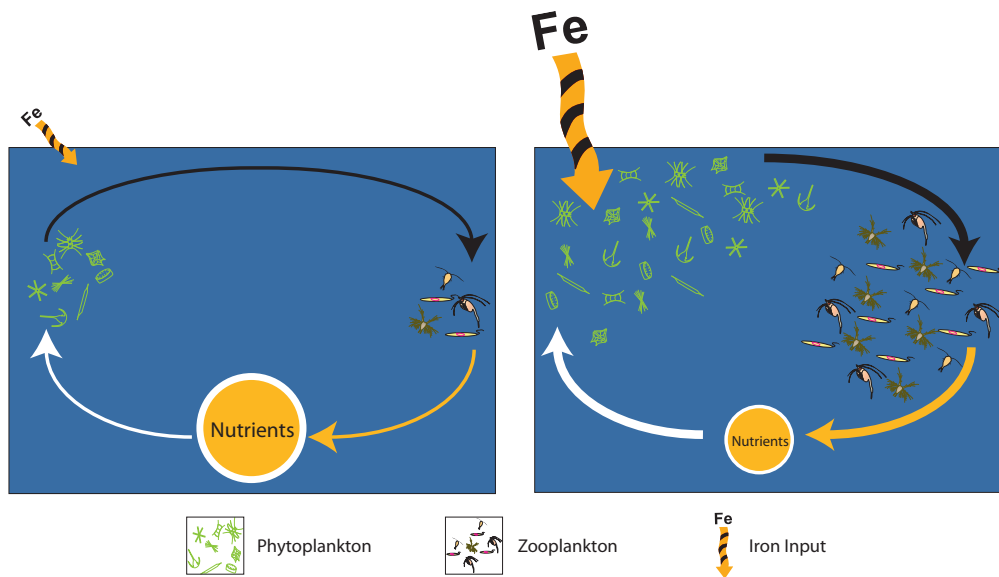


**Figure 4.9** Limitation of phytoplankton production due to low concentrations of iron (Fe) and subsequent effects on zooplankton. This situation occurs in the Pacific Equatorial Divergence province, where iron limitation occurs in the presence of significant levels of macronutrients. Such limitation, combined with a balance between prey and their consumers, characterises the ‘High Nutrient-Low Chlorophyll’ (HNLC) systems of the world’s oceans.

#### 4.4.2 Western Pacific Warm Pool

During average climatic conditions, the biomass of both phytoplankton and heterotrophs in the photic zone of the Warm Pool is only half that in PEQD (Figure 4.10b). The biomass of heterotrophic bacteria and microzooplankton in the deeper layers remains unknown. However, an intriguing feature of the Warm Pool is that the composition of phytoplankton found at the base of its mixed layer is similar to that of the upper water column in PEQD<sup>12</sup>. This suggests that there may be some continuity between the deeper layer of the Warm Pool and the surface layer of PEQD in the ‘transition zone’ that stretches across ~ 15 degrees of longitude (1700 km) to the west of the front between the two provinces.

If the same continuity applies to organic matter synthesised in PEQD, this would mean bacteria and detritivorous zooplankton would be available in the Warm Pool to support the larger zooplankton and micronekton that provide prey for tuna. Such a mechanism would explain the relatively high biomass of micronekton in the Warm Pool (Figure 4.10b), and the fact that tuna are often abundant there (Chapter 8). At this stage, however, we are lacking data on processes at the front between PEQD and the Warm Pool, and the ‘transition’ zone between the two provinces that frequently undergoes shifts in longitude (Chapter 3).

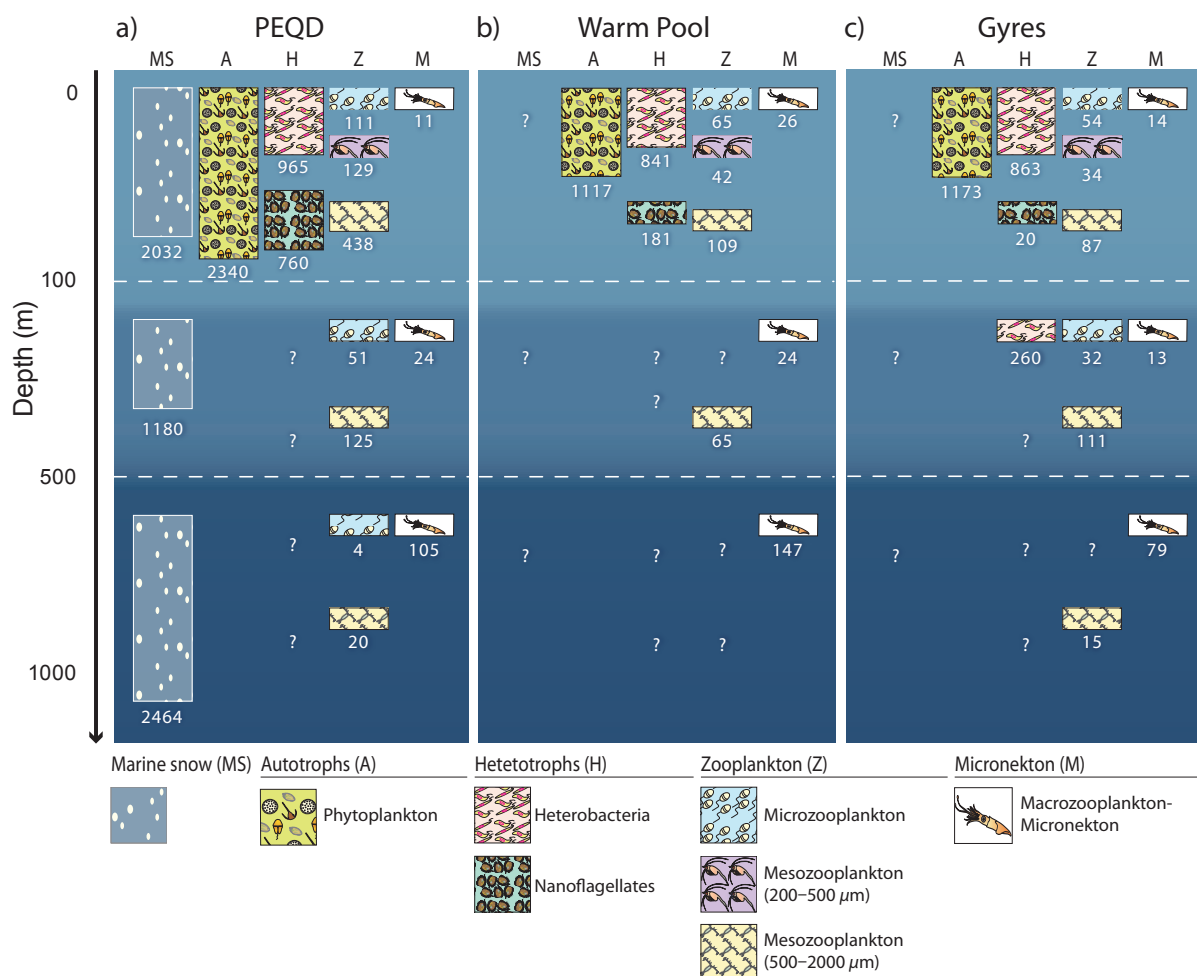


**Figure 4.10** Structure of the food webs in (a) the Pacific Equatorial Divergence province along the equator; (b) the Warm Pool along the equator; and (c) the North Pacific Tropical Gyre and South Pacific Subtropical Gyre. Boxes and the figure below them indicate the mean daily biomass of the different components of the ecosystem (in mg carbon per m<sup>2</sup>), i.e. taking diel vertical migrations into account. The mesozooplankton biomass below the photic zone (100 m) refers to the sum of the two size fractions (200–500 and 500–2000 μm). ? = no data available (source: Legand et al. 1972, Brown et al. 2003, Gorsky et al. 2003, Hidaka et al. 2003, Ishizaka et al. 1997, Le Borgne et al. 2003, Roman et al. 1995, Le Borgne and Rodier 1997, Le Borgne and Landry 2003)<sup>22,38,39,70,104,105,127–129</sup>.

Interannual variations in the vertical structure of the Warm Pool due to ENSO (Section 4.3.2) have a major effect on the food web. During El Niño episodes, the shallower thermocline results in 7.7 times more new production<sup>40</sup>. Consequently, total primary production more than doubles<sup>41</sup> and the biomass of zooplankton is 1.5 times higher. When combined with the increase in the surface area of the Warm Pool during El Niño, the overall productivity of this province is enhanced significantly. Indeed, the increased productivity is probably greater than indicated on the basis of ocean colour imagery because remote sensing of the surface layer does not detect the important components of the food web located in the deeper layers.

### 4.4.3 North Pacific Tropical Gyre and South Pacific Subtropical Gyre

Based on the concentrations of chlorophyll *a* in surface waters evident in ocean colour images, NPTG and SPSG appear to be among the largest and most oligotrophic oceanic provinces in the world<sup>42</sup>. However, as described for the Warm Pool, this view needs to be tempered to some extent because important biological processes take place much deeper than indicated by remote sensing of the surface layer. Plankton biomass is at a minimum in the centres of these gyres<sup>43</sup>. Overall, the biomass of heterotrophic bacteria and phytoplankton in the photic zone is similar to the biomass in the Warm Pool, although it is significantly lower for microzooplankton, particularly nanoflagellates (Figure 4.10c). Reductions in microzooplankton and mesozooplankton for a similar biomass of phytoplankton indicate that there are more trophic links between the phytoplankton and the zooplankton in NPTG and SPSG than in the Warm Pool. This is because energy losses occur during each transfer from prey to consumers, with the result that complex food webs, with more trophic links, are less efficient in producing zooplankton and, above all, top predators, from a given biomass of phytoplankton.

The nutrient-poor nature of these two gyres is due to their vertical structure. Both gyres are regions of downwelling, so that the only way for nutrients to reach the photic zone is by mixing of the deeper nutrient-rich layers with shallower waters, and by eddy diffusion. Moreover, because nitrate concentrations in the deep layers are ~ 3 times lower than in the equatorial area (PEQD and Warm Pool) (Figure 4.7), the transfers of nutrients are correspondingly small when mixing and diffusion occur.

The low rate of nutrient transfer to the surface waters of the gyres is reduced further by the formation of a marked thermocline during summer (Section 4.3.3), leading to a decrease in phytoplankton biomass in SPSG<sup>1</sup>. However, this summer minimum may be masked by development of *Trichodesmium* blooms in the surface layer of the southwestern Pacific<sup>45</sup>. In addition to these seasonal fluctuations in the food webs of the gyres, there are similar interannual variations in phytoplankton<sup>44,46</sup> and the biomass of micronektonic fish<sup>47</sup> in NPTG.

### 4.4.4 Archipelagic Deep Basins

The food webs for tuna and other large pelagic fish in ARCH are based on two sources of nutrients: runoff from high islands, and the mesoscale physical processes described in Section 4.3.4. They also rely on biological linkages between species associated with islands and tuna in the open ocean.

High islands discharge large quantities of sediment and nutrients into the surrounding ocean (Chapter 7), leading to a gradient of increased biological productivity from inshore to offshore<sup>48,49</sup>. In contrast, productivity in the open ocean close to coral atolls and banks is rarely enhanced<sup>50,51</sup> because these low-lying islands

release very few sediments and nutrients, with the exception of those from aquifers<sup>52</sup>. Temporal variations in sediment and nutrient inputs from high islands are linked to seasonal and interannual patterns of rainfall (Chapters 2 and 7). Higher food web biomass should, therefore, occur around the islands and archipelagos during the rainy season, i.e. in summer. Indeed, a summer maximum has been observed from ocean colour imagery, attributed to *Trichodesmium* blooms in the New Caledonia and Vanuatu archipelagos<sup>53</sup>. No effect has been observed on subsurface planktonic biomass, however, particularly at secondary and tertiary levels<sup>50</sup>.



A *Trichodesmium* bloom

Photo : Chris Roelfsema

Among the mesoscale processes, eddies are the most common. Cyclonic eddies, which bring more nutrients into the photic zone (Chapter 3), have some of the greatest effects on primary productivity. Anticyclonic eddies, however, suppress upward mixing of nutrients, as described earlier for NPTG and SPST. Although they are not within ARCH, the cyclonic eddies in the Hawaiian archipelago provide a good example of the benefits of these particular mesoscale processes – they uplift nutrient-rich waters by 30 to 140 m, increasing chlorophyll *a* concentration by 1.1 to 5 times<sup>54</sup>. Corresponding variations also occur for other components of the food web, such as microzooplankton<sup>55</sup> and mesozooplankton<sup>56</sup>.

Upwellings induced by the divergence of currents around island barrier reefs or coastal zones also deliver more nutrients to supply food webs in some parts of ARCH. This has been observed in southwestern New Caledonia<sup>57</sup>, although enrichment of the surface layer there in summer is limited because nutrient concentrations in the source water are very low<sup>58</sup>.

Concentrations of chlorophyll *a* and zooplankton may be higher just above seamounts due to other mesoscale processes<sup>59,60</sup>, leading to local increases in nutrients in surface waters. Such physical processes may be visible in oceanographic data as a ‘doming’ of the hydrographical structure<sup>61</sup>. Other processes, such as changes in current regimes around seamounts, can also lead to differences in the abundance and behaviour of micronekton between the seamount and the surrounding ocean<sup>62,63</sup>. In addition, increased amplitude of internal waves in shallow water affects the vertical distribution of phytoplankton<sup>64</sup> and can cause aggregation of this primary food source.

The linkages between islands and continental slopes, and food webs for tuna, can occur via the planktonic phase of coral reef fish, and via micronekton. Postlarvae originating from populations of coral reef fish and invertebrates are often entrained in eddies while they develop to the stage where they are competent to settle on reefs<sup>65</sup> (Chapter 9), and have been recorded from the stomach contents of tuna<sup>66</sup>. Mesopelagic micronekton have a distinct species composition at depths of 400 to 700 m in the vicinity of islands and continental slopes<sup>67,68</sup>, indicating that these micronekton represent a distinct source of food for tuna.

The high spatial and temporal variability in primary production makes it impractical to present a ‘typical’ structure for food webs in ARCH. The variation of food webs across the province is illustrated by changes in phytoplankton and mesozooplankton collected at 19 sites near New Caledonia (Figure 4.11). Phytoplankton biomass ranged from 16 to 35 mg chlorophyll *a* units per m<sup>2</sup> for the photic zone (0–120 m), and zooplankton biomass varied from 190 to 330 mg carbon (C) per m<sup>2</sup> for the upper 200 m of the water column. The lower values approximate those from the most oligotrophic regions of the tropical Pacific Ocean, whereas the higher values are slightly lower than in PEQD. No offshore-inshore gradient is apparent<sup>50</sup>, a pattern that is also true for the macrozooplankton and micronekton near New Caledonia<sup>51</sup>.

#### **4.4.5 Overview of differences in food webs among provinces**

Some simple comparisons help to highlight the main differences in the food webs for tuna among the five provinces. The ratio of phytoplankton biomass to mesozooplankton biomass is an indicator of the complexity of a food web: food webs based on large phytoplankton supported by ‘new’ nutrients have fewer trophic links because the herbivores that feed on this phytoplankton are larger. In particular, there is a direct link, or only one intermediate trophic link, between phytoplankton and mesozooplankton. As a result, the ratio between the biomass of phytoplankton and zooplankton is rather low. Based on data in Figure 4.10, this ratio varies from 4.1 in PEQD, to 7.4 in the Warm Pool and to 9.7 for the gyres, indicating the existence of more trophic links between phytoplankton and mesozooplankton in the oligotrophic ecosystems (Warm Pool and gyres) than in PEQD. For the reasons explained in Section 4.4.4, the ratio varies greatly within ARCH. In short, a greater biomass of phytoplankton is needed for a given mesozooplankton biomass in oligotrophic systems.

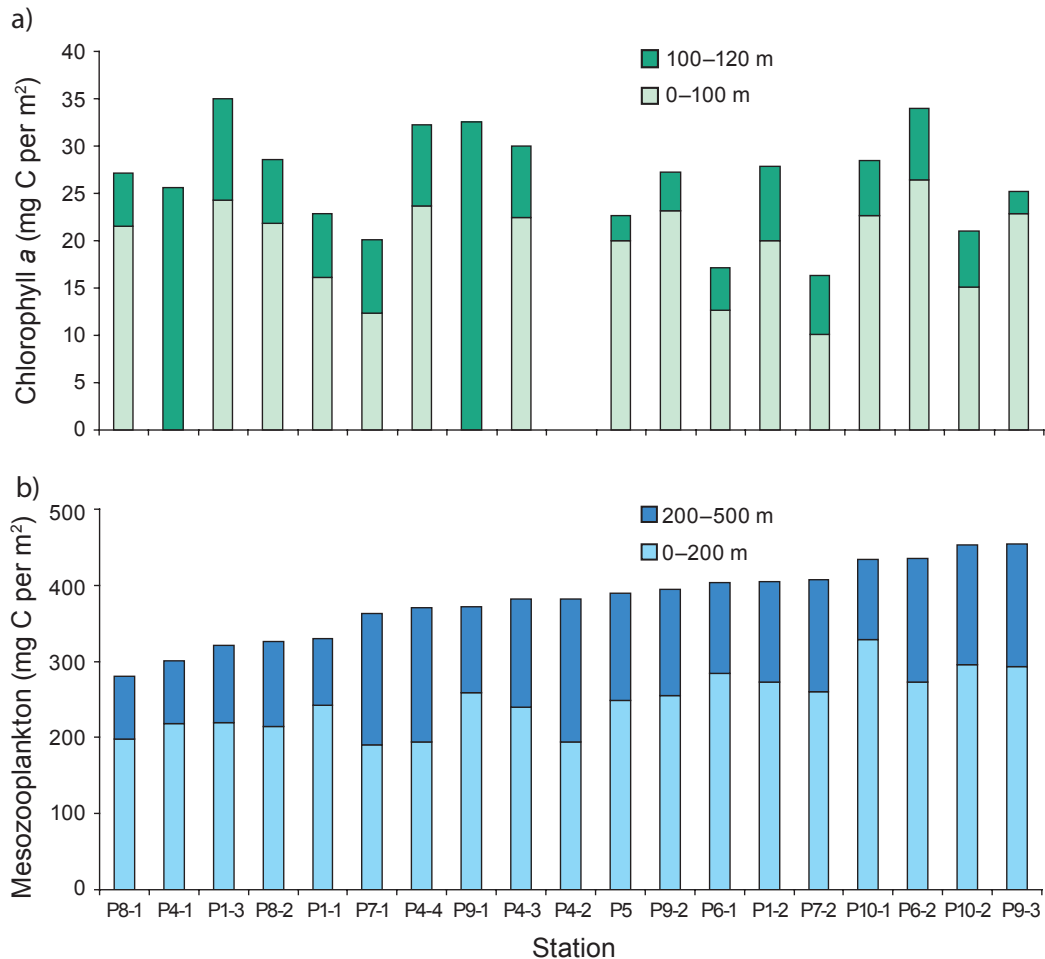


**Figure 4.11** Biomass of (a) phytoplankton and (b) mesozooplankton at 19 oceanographic stations in New Caledonia. Sampling at these stations lasted for at least 24 hours to account for any day/night variation in abundance (source: Institut de Recherche pour le Développement)<sup>75</sup>.

Interestingly, ratios between the total biomass of primary producers and total heterotrophic biomass are very close in the different provinces (0.9 in the Warm Pool, 1.0 in PEQD and 1.1 in the gyres). This is because a given phytoplankton biomass supports about the same heterotrophic biomass. The composition of the heterotrophs may change, however, with more heterotrophic bacteria and nanozooplankton occurring in oligotrophic ecosystems. The food webs in all provinces, except ARCH, are in a relatively steady state on short- to mid-term time scales (weekly to seasonal periods). In ARCH, short-term physical forcing due to the range of mesoscale processes, leads to an unbalanced ecosystem, with variable ratios between phytoplankton and heterotrophs. While nutrient inputs to the photic zone are more or less constant in the other provinces, they are quite variable over time within ARCH, creating a time lag of several days between the inputs and the subsequent responses

of primary productivity and grazing by zooplankton. This means that there is often little correlation between the various levels of the food web in ARCH at any given time.

Comparisons between the deep and surface layers also help to distinguish the food webs from different provinces. For example, the biomass of mesozooplankton down to a depth of 1000 m in PEQD is 3.3 times greater than in the gyres, and the biomass of micronekton is 1.9 times greater. The reason is that most of the mesozooplankton is closely linked to the photic zone in PEQD, whereas part of the micronekton lives permanently at a depth of 500 to 1000 m and depends on different trophic pathways. Thus, only 16% of the micronekton biomass within the depth range 0 to 1000 m is in the photic zone at night in PEQD<sup>22</sup>, whereas 40% occurs there in the gyres<sup>69</sup>, 44% in ARCH<sup>51</sup> and 50% in the Warm Pool<sup>70</sup>. The taxonomic composition of micronekton is consistent among provinces, however, and includes fish, squid, and carid, sergestid, penaeid and euphausiid shrimp.

It is not yet possible to identify relationships between micronekton biomass and mesozooplankton biomass among provinces, although it appears that ratios between the two biomasses vary considerably, ie 0.18 (PEQD), 0.91 (Warm Pool) and 0.38 (SPSG and NPTG). Several sources of variability need to be quantified to estimate these ratios more accurately. These include (1) the influence of lateral transport of micronekton between provinces, particularly between PEQD and the Warm Pool; (2) the time lag and spatial drift affecting phytoplankton, mesozooplankton and micronekton biomasses; and (3) the differences in complexity of food webs among provinces, especially the amount of micronekton and mesozooplankton derived from a given biomass of phytoplankton.

## **4.5 Critical requirements for maintenance of food webs in each province**

The food web in each province operates differently – it is constrained by lack of macronutrients in the Warm Pool and the gyres, and by iron and, to a lesser extent, by silicate in PEQD<sup>11</sup> (Section 4.3.1). We briefly reiterate these constraints here, and indicate the factors most likely to affect the productivity of the food webs in each province if they are altered by climate change.

### **4.5.1 Macronutrients and micronutrients**

Major nutrients (or macronutrients) are the main limiting factor in the Warm Pool, NPTG, SPSG, and ARCH. Nitrogen in the form of ammonium, urea or nitrate is particularly important, except for diazotrophic organisms like *Trichodesmium* (Section 4.2.2). Availability of new nitrogen, mediated by the vertical structure of the water column, and processes like upwelling and eddies, or mesoscale processes in the case of ARCH, determine the diversity and richness of the food webs for tuna in

these provinces. Diazotrophs, on the other hand, require a different mix of elements, including phosphorus and iron<sup>15</sup>. Whether phosphorus or iron is the primary limiting element depends on the area considered. For example, only phosphorus limits diazotrophy in New Caledonia at the end of summer because iron concentrations are high then due to runoff<sup>71</sup>.



Photos: Céline Barré

Sampling zooplankton and filtering phytoplankton

In PEQD, iron is the limiting factor. The importance of iron limitation in PEQD led to two mesoscale iron experiments (IronEx I and II) in the equatorial Pacific in October 1993 and May–June 1995<sup>72</sup>. During IronEx II, infusion of iron was followed by a bloom of phytoplankton and, subsequently, a higher biomass of microzooplankton<sup>73</sup>. Mesozooplankton did not respond within the duration of the experimental observations, however, possibly due to a lack of viable young or an abundance of predators<sup>74</sup>. The consequences of iron enrichment on oceanic food webs are still poorly understood, in part because of the small spatial scale of experiments conducted to date.

#### 4.5.2 Temperature

Adequate water temperatures are needed for the efficient metabolism of planktonic organisms. Temperature determines the turnover rates of organisms living in the mixed layer. The warm water temperatures in the tropical Pacific result in short turnover times for phytoplankton biomass in the photic zone: 1.7 days in PEQD, 1.6 to 4.4 days in the Warm Pool and 3.8 days in the gyres<sup>75</sup>. At the top of the food web, all the tuna species have a wide but variable thermal tolerance (Chapter 8), allowing them to occupy a range of depths in much of the area covered by the five provinces. However, the micronekton on which tuna feed are less mobile and/or

more restricted physiologically. They are potentially more susceptible to changes in physical conditions resulting from ocean warming. Overall, however, changes in temperature are likely to have their greatest influence on food webs for tuna through their effects on the vertical structure of the water column (i.e. stratification), rather than directly on planktonic organisms. After all, most zooplankton and micronekton are able to cope with drastic thermal changes during vertical migrations (Box 4.2).

### 4.5.3 Dissolved oxygen

Low concentrations of dissolved oxygen, such as those found in the equatorial convergence zones (Figure 4.8), are a limiting factor for aerobic organisms, particularly micronekton. The low biomass of micronekton in PEQD, compared with areas located to the south, may be due to low oxygen concentrations beneath the photic zone of this province, despite the higher productivity within it<sup>69</sup>. However, some mesopelagic species can tolerate waters with very low oxygen concentrations during their diel cycle, and some of them actually reside within these areas, e.g. copepods in the genus *Lucicutia*<sup>76</sup>.

### 4.5.4 Solar radiation

Solar radiation is absorbed and scattered in the ocean and light, therefore, declines exponentially with depth. Phytoplankton cells have the potential to photo-acclimate, having a lower pigment content near the sea surface. Conversely, phytoplankton found at the lower limit of the photic zone have a higher pigment content per cell, which contributes to the deep chlorophyll maximum (DCM), found at ~ 50 m in PEQD (Figure 4.7) – note that this is not a biomass maximum nor a production maximum in most instances. Despite ample nutrients, maximum productivity of phytoplankton in PEQD occurs at 30 m and not at the surface due to photo-inhibition. Because light intensity decreases exponentially with depth, spatial and temporal variations in incident solar energy can be expected to affect the vertical distributions of phytoplankton maxima only very slightly. The effects of solar radiation are not as profound for some zooplankton. For example, the cnidarian *Velella velella*, the mollusc *Janthina* sp. and pontellid copepods have developed blue protective pigments to enable them to live at the surface.

### 4.5.5 Carbon dioxide

The partial pressure of carbon dioxide ( $p\text{CO}_2$ ) in the ocean has direct and indirect effects on pelagic organisms. Increasing  $p\text{CO}_2$  may also increase diazotrophy, because there is some evidence that growth of *Trichodesmium* increases at higher concentrations of carbon<sup>77</sup>. This increase in diazotrophy, provided iron and SRP limitations are alleviated, is expected to change the structure of the ecosystem, particularly the relative abundance and species composition of grazers and microbial populations.

Although the nature of these changes is unknown, it is certain that changes in  $p\text{CO}_2$  will alter biological communities<sup>77</sup>. An increase in  $p\text{CO}_2$  is also likely to exacerbate the effects of low oxygen concentrations on organisms living in the deep ocean<sup>78</sup>.

Phytoplankton (haptophytes) and zooplankton (e.g. pteropods) that use calcium carbonate to build their shells also depend on  $p\text{CO}_2$  in the ocean staying within a certain range. If it increases, the pH of the ocean decreases, limiting the availability of carbonate ions [ $\text{CO}_3^{2-}$ ] for constructing shells<sup>79</sup> (Chapter 3). However, the effects of ocean acidification are complex because pelagic organisms have to face other environmental changes simultaneously (temperature, nutrient supply) and ecosystem constraints (competition, grazing pressure).



Pteropod from the tropical Pacific

Photo: Photoshot/SuperStock

#### 4.6 Recent observed changes in the food webs of provinces

The extent of recent changes to the food webs in each province are relatively poorly known because there have been few long-term observations of oceanic ecosystems in the region. Instead, far more emphasis has been placed on monitoring the physical features of the tropical Pacific Ocean. Most of our present knowledge comes from (1) satellite remote sensing of phytoplankton biomass based on pigments in the surface layer down to a depth of 20 m in oligotrophic regions; and (2) a single station in NPTG, the Hawaii Ocean Time-Series (HOT), outside our main area of interest. Therefore, we have had to make some inferences from more global information.

Ocean colour satellite imagery from two periods, 1979 to 1986 and 1997 to 2000, shows that surface chlorophyll *a* concentrations in the oligotrophic oceans of the world decreased by 8% from the early 1980s to the late 1990s<sup>80</sup>. More recently, a 9-year time-series of ocean colour data (1998–2006) shows that ocean gyres with chlorophyll *a* concentrations < 0.07 mg per m<sup>3</sup> appear to be expanding rapidly<sup>42</sup>. The area of these gyres increased by 2.2% per year over this period in the northern Pacific, and by 1.4% in the southern Pacific. There was also a corresponding increase in sea surface temperature of the gyres in the northern and southern Pacific of 0.014°C per year and 0.02°C per year, respectively. This lends support to the hypothesis that increased stratification leads to lower primary productivity (Section 4.3.3 and Chapter 3). There is also some evidence that abundance of zooplankton at the surface has declined in the tropical north Atlantic<sup>81</sup>.

Samples taken throughout the water column at the HOT station do not reflect the global trend that the planktonic biomass appears to be decreasing. Rather, the data show that primary production increased by 50% in the last 20 years<sup>82</sup> as a result of the influence of ENSO and the Pacific Decadal Oscillation (PDO) (Chapter 2) on upper ocean stratification and the delivery of nutrients. However, there has been an increase in chlorophyll *b*, suggesting a shift towards an ecosystem dominated by cyanobacteria. The biomass of mesozooplankton also increased between 1994 and 2006 (Figure 4.12). Although the length of the time-series from Hawaii is still relatively short, it indicates that enhanced stratification and decreased nutrient availability has resulted in selection for N<sub>2</sub>-fixing cyanobacteria (including *Trichodesmium*), and a shift to conditions where phosphorus or iron limit the growth of phytoplankton. These regime shifts are linked to changes in the PDO sign, independently of trends, which happen on a much longer time-scale (50–100 years).

Changes in the extent of low-oxygen zones at intermediate depths have also occurred in the last 50 years in tropical oceans, including the eastern equatorial Pacific (Chapter 3). Although this has obvious implications for micronekton, no comparisons of the vertical distributions over time have been made for this important source of prey for tuna.

## 4.7 Projected changes to the environment and food webs of provinces

Except for one modelling study<sup>83</sup>, information about expected changes to the main features of the tropical Pacific Ocean is not always available at the level of the ecological provinces (Chapter 3). To help assess the vulnerability of the food webs in each province to climate change, we modelled the projected effects of the B1 and A2 emissions scenarios for 2035 and 2100 on the surface area, mixed layer depth and other physical and chemical features of all five provinces. Projections were made for the range of physical and chemical variables from the IPSL coupled 3-D atmosphere-

ocean climate model (also used in Chapter 8 and included in the ensemble of models used in Chapter 3). Latitude ranges and concentrations of nutrients were used to define the boundaries of provinces in the model (Table 4.2).

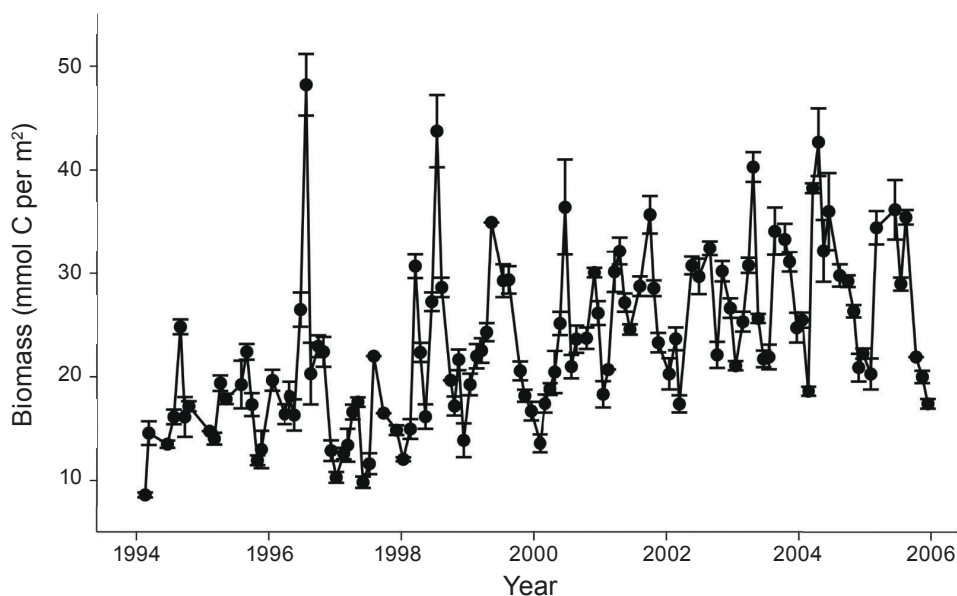


**Figure 4.12** Variation in the biomass of mesozooplankton at the Hawaii Ocean Time-series (HOT) station between 1994 and 2006, showing an increasing trend (source: [www.hahana.soest.hawaii.edu/hot/hot-dogs/mseries.html](http://www.hahana.soest.hawaii.edu/hot/hot-dogs/mseries.html), Decima et al. 2010)<sup>130</sup>.

The projected changes to the physical and chemical nature of each province were then incorporated into a biogeochemical model (Pelagic Interaction Scheme for Carbon and Ecosystem Studies, PISCES)<sup>84</sup> to assess the likely responses of phytoplankton and zooplankton. Forecasting changes in food webs, using a multi-model mean from an ensemble analysis, similar to the approach used for the physical climate models in Chapter 3, was not possible due to the limited development of biogeochemical models.

The PISCES model simulates the cycling of carbon, oxygen and the major nutrients needed for phytoplankton growth (e.g. nitrate, SRP, silicate). The model has two phytoplankton size classes; one representing picophytoplankton and nanophytoplankton (Table 4.1) and the other for the larger phytoplankton (diatoms).

It also has two zooplankton size classes, representing nanozooplankton and microzooplankton for the small size, and mesozooplankton for the larger one. Phytoplankton growth is limited by the availability of nutrients, temperature and light. Iron is supplied to the ocean by aeolian dust and runoff. The sink of iron needed to balance sources of iron is simulated by scavenging of iron onto particulate

organic matter. There are two non-living components of particulate organic carbon in the model (small and large) and one for dissolved organic carbon. The model results are based on the IPSL-CM4-LOOP simulations<sup>7</sup>.

**Table 4.2** Information used to define the boundaries of the five ecological provinces in the modelling described in Section 4.7.

| Province  | Latitude range                   | Surface nitrate concentration threshold ( $\mu\text{M}$ ) |
|-----------|----------------------------------|---|
| PEQD      | 10°S–10°N                        | > 0.1   |
| Warm Pool | 6°S–9°N                          | < 0.1   |
| NPTG      | 9°N–30°N                         | < 0.1   |
| SPSG      | 6°S–45°S                         | < 0.1   |
| ARCH      | Fixed region given in Figure 4.6 |   |

PEQD = Pacific Equatorial Divergence; Warm Pool = Western Pacific Warm Pool; NPTG = North Pacific Tropical Gyre; SPSG = South Pacific Subtropical Gyre; ARCH = Archipelagic Deep Basins.

The results of modelling the projected physical and chemical changes to each province are summarised in the next section, whereas the projections for changes in phytoplankton and zooplankton are presented in Section 4.9.

#### 4.7.1 Projected changes to key physical and chemical features of provinces

The modelled projections of the effects of climate change on the surface areas of provinces under the B1 and A2 emissions scenarios show three main trends. First, a reduction of the area of PEQD as its western border is displaced eastward. A reduction of 20–27% in surface area is expected by 2035, with the western edge of the province moving from 180° to 170°W. A 30% shrinkage of the province is projected to occur under B1 and a 50% decrease under A2 by 2100, with the western edge lying between 160°W and 150°W (Figure 4.13, Table 4.3). Second, a corresponding increase in the area of the Warm Pool, which is expected to expand by 18–21% in 2035 and by 26% and 48% under B1 and A2, respectively, by 2100 (Figure 4.13, Table 4.3). Such variations are less than those reported in Chapter 3 because our definition of the Warm Pool province is based on surface nitrate levels, which is a better definition for the biological productivity projections than temperature and salinity. Third, the gyres are expected to expand towards the poles and to the west (Figure 4.13, Table 4.3). This expansion will be greater for SPSG, where the oligotrophic waters are expected to increase by 4–7% in 2035, and up to 14% for the A2 scenario by 2100 (Figure 4.13, Table 4.3). No change in the area of ARCH is expected, by definition.

For all provinces, the average mixed layer depth (MLD) is projected to decrease by < 10% for both scenarios in 2035 and 2100 except for PEQD (Table 4.3). The decreases in MLD in the Warm Pool are expected to have little effect on the supply of nutrients to the photic zone due to the strong gradient of the thermocline there, as outlined in Section 4.3.2. However, for the gyres (Case 3, Figure 4.3), a decreasing MLD is

expected to reduce nutrient inputs into the photic zone, because the gradient gets stronger as it usually occurs during summer. In PEQD, the greater decreases in MLD projected to occur by 2100 (Table 4.3) are not expected to affect primary production because nitrate concentrations there, due to upwelling, are still likely to exceed levels at which the supply of iron presently limits the growth of phytoplankton.

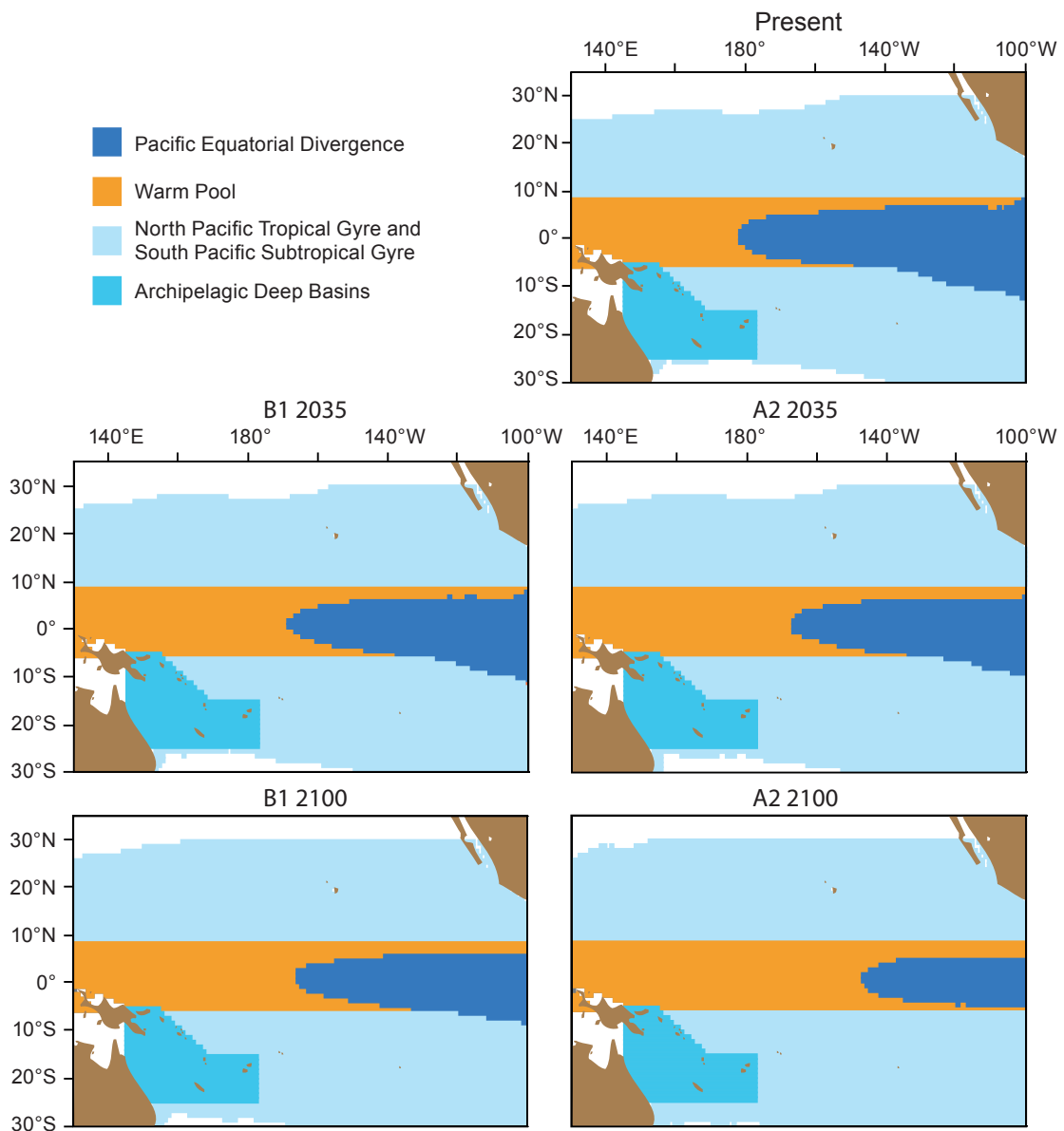


**Figure 4.13** Projected changes in surface areas of the five ecological provinces in the tropical Pacific Ocean under the B1 and A2 emissions scenarios for 2035 and 2100, relative to present conditions.

The modelling also shows ubiquitous warming of the region (Table 4.3), which is expected to increase stratification (Chapter 3) and inhibit the supply of nutrients to the surface in oligotrophic provinces. Although the greatest warming is projected to occur in the non-upwelling areas of the equatorial Pacific, the enhanced warming of the equatorial region in general is expected to reduce the upwelling of deep, nutrient-rich water, contributing to the contraction of PEQD. This contraction is most pronounced in the A2 scenario (Figure 4.13) and helps explain why NPP is expected to decrease across the entire equatorial Pacific by 2100 under high emissions of CO<sub>2</sub><sup>85</sup>.

Dissolved oxygen (O<sub>2</sub>) is projected to decrease by up to 26% in PEQD to a depth of 300 m by 2100 under the A2 scenario, and increase by 7–8% in NPTG by 2100 under the B1 and A2 scenarios (Table 4.3). Elsewhere, changes to O<sub>2</sub> at 300 m are minor and, in all provinces except PEQD, percentage saturation of O<sub>2</sub> is expected to be 50–75%. In PEQD, however, it is projected to drop to 22–28%.

Few differences in the effects of ocean acidification are expected among provinces measured using Omega aragonite ( $\Omega$  aragonite) (Chapter 3). Depending on the emissions scenario, the projected decrease of  $\Omega$  aragonite ranges between 8% and 35% (Table 4.3), which corresponds to a diminution in calcification rates of 2–9% for corals<sup>86</sup>. For pelagic organisms like haptophytes, the response to ocean acidification is less clear<sup>87,88</sup>, with responses ranging from increased growth and calcification<sup>89</sup> to moderate decrease in growth and calcification.

## 4.8 Projected vulnerability of food webs in provinces

To assess the vulnerability of food webs for tuna and other large pelagic fish in each province, we have applied the vulnerability framework described in Chapter 1. This framework is based on (1) exposure to changes in the key physical and chemical features of the environment; (2) the sensitivity of all levels in the food web to this exposure; (3) the potential impact of this exposure and sensitivity; and (4) the capacity of the organisms to adapt to these changes and reduce the potential impact.

We have assessed the vulnerability of food webs in each province to changes in water temperature, mixed layer depth, nutrient inputs to the photic zone, solar and ultraviolet radiation, dissolved oxygen and ocean acidification. Exposure to these variables is based on the assessments of how they are projected to change according to the modelling described in Section 4.7, and the assessments in Chapter 3.

### 4.8.1 Water temperature

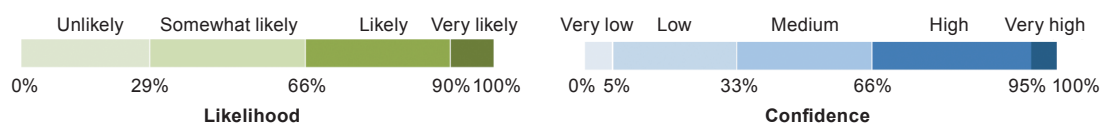
#### *Exposure and sensitivity*

As described in Chapter 3, sea surface temperatures (SSTs) are projected to increase by 0.7–0.8°C by 2035 under both the B1 and A2 emissions scenarios across the region. By 2100, SSTs are expected to be 1.4°C greater under B1, and increase by 2.5°C for A2.

**Table 4.3** Projected effects of the B1 and A2 emissions scenarios for 2035 and 2100 on the main physical, chemical and biological features of the five ecological provinces in the tropical Pacific Ocean (based on the IPSL/PISCES model). Values are percentage changes relative to present values (2000–2010). Numbers in brackets refer to actual projected changes in SST (°C); actual projected MLD (m); actual projected percentage saturation of O<sub>2</sub> at a depth of 300 m; and actual projected aragonite saturation state ( $\Omega$ , no unit). Likelihood and confidence values for each projection can be estimated for each cell in the table by combining the likelihood values for scenarios and the confidence values for features of the province.

| Province  | Year | Scenario | Feature of Province |          |          |                |                    |     |            |
|-----------|------|----------|---------------------|----------|----------|----------------|--------------------|-----|------------|
|           |      |          | Area                | SST      | MLD      | O <sub>2</sub> | $\Omega$ aragonite | NPP | ZooBiomass |
| PEQD      | 2035 | B1       | -20                 | +1 (0.3) | -5 (24)  | -8 (26)        | -10 (3.43)         | 0   | -2         |
|           |      | A2       | -27                 | +2 (0.5) | -9 (24)  | -12 (26)       | -9 (3.51)          | 0   | -2         |
|           | 2100 | B1       | -30                 | +3 (0.9) | -12 (23) | -5 (28)        | -15 (3.24)         | +2  | -3         |
|           |      | A2       | -50                 | +6 (1.6) | -26 (19) | -26 (22)       | -35 (2.49)         | +4  | -6         |
| Warm Pool | 2035 | B1       | +18                 | +1 (0.4) | +3 (32)  | 0 (50)         | -8 (3.82)          | -7  | -6         |
|           |      | A2       | +21                 | +2 (0.5) | -5 (27)  | -2 (49)        | -10 (3.74)         | -5  | -3         |
|           | 2100 | B1       | +26                 | +4 (1.2) | 0 (30)   | 0 (50)         | -17 (3.46)         | -9  | -9         |
|           |      | A2       | +48                 | +7 (2.3) | -5 (29)  | -2 (49)        | -33 (2.79)         | -9  | -10        |
| NPTG      | 2035 | B1       | +1                  | +1 (0.0) | -2 (37)  | +1 (61)        | -8 (3.57)          | -3  | -3         |
|           |      | A2       | +1                  | +1 (0.4) | -3 (36)  | +3 (60)        | -11 (3.66)         | -5  | -4         |
|           | 2100 | B1       | +1                  | +5 (1.3) | -1 (37)  | +7 (63)        | -18 (3.27)         | -11 | -10        |
|           |      | A2       | +1                  | +9 (2.4) | -3 (36)  | +8 (64)        | -33 (2.66)         | -22 | -18        |
| SPSG      | 2035 | B1       | +4                  | +2 (0.5) | 0 (40)   | -2 (66)        | -8 (3.69)          | -3  | -3         |
|           |      | A2       | +7                  | +2 (0.5) | -5 (38)  | -4 (65)        | -11 (3.60)         | -5  | -4         |
|           | 2100 | B1       | +7                  | +4 (1.1) | 0 (40)   | -2 (66)        | -18 (3.32)         | -3  | -5         |
|           |      | A2       | +14                 | +8 (2.1) | -6 (39)  | -4 (64)        | -34 (2.65)         | -6  | -10        |
| ARCH      | 2035 | B1       | 0                   | +2 (0.5) | -3 (38)  | -1 (75)        | -9 (3.77)          | -5  | -5         |
|           |      | A2       | 0                   | +2 (0.5) | -3 (37)  | -3 (74)        | -12 (3.69)         | -8  | -6         |
|           | 2100 | B1       | 0                   | +5 (1.3) | -7 (36)  | -1 (75)        | -18 (3.38)         | -20 | -17        |
|           |      | A2       | 0                   | +9 (2.4) | -9 (35)  | -1 (75)        | -35 (2.70)         | -33 | -26        |

Area = surface area of the province; SST = sea surface temperature; MLD = mixed layer depth; O<sub>2</sub> = dissolved oxygen at a depth of 300 m;  $\Omega$  aragonite = Omega aragonite; NPP = net primary production; ZooBiomass = zooplankton biomass; PEQD = Pacific Equatorial Divergence; Warm Pool = Western Pacific Warm Pool; NPTG = North Pacific Tropical Gyre; SPSPG = South Pacific Subtropical Gyre; ARCH = Archipelagic Deep Basins.



The projected increases in SST at the scale of provinces derived from the IPSL model used here show a similar trend, although warming of all provinces is expected to be limited to 0.5°C by 2035, and warming of PEQD by 2100 is lower than for the other provinces (Table 4.3).

Higher SSTs are expected to increase stratification of the water column, with a greater temperature gradient in the thermocline and reduced exchanges between the mixed layer and the colder water below. This has implications for the transfer of nutrients for new primary production in the photic zone for all provinces (see below). However, here we focus on the direct effects of temperature on the organisms that comprise the food webs for tuna.

Temperature affects the metabolism of single-cell plants and animals, and larger animals with a variable body temperature (poikilotherms). Most experiments on the effects of temperature on metabolic rates have shown an exponential increase until a peak is reached, followed by a decreasing trend. The increasing phase follows the same law as the velocity of chemical reactions with temperature (Arrhenius' law) and is characterised by the  $Q_{10}$  index, i.e. the slope of the curve to the power 10. Present knowledge of the  $Q_{10}$  value for animals in the food webs for tuna is based mainly on cultures or short incubations of organisms collected from the natural environment – longer-term responses of organisms to increased temperatures remain poorly understood.

In phytoplankton<sup>90</sup>, cyanobacteria<sup>91</sup> and copepods<sup>92</sup>, the effects of increases in temperature lead to higher metabolic capacities, which depend on the metabolic function involved. For example, the  $Q_{10}$  of copepods differs for respiration, nitrogen and phosphorus excretions, assimilation, and production rates. In general, respiration increases more rapidly with temperature than excretion for a given food concentration, resulting in greater use of carbohydrates and lipids<sup>92</sup>, with the result that temperature affects the growth efficiency of the copepods. The sensitivity of cyanobacteria and copepods also depends on the species involved and their life stage, and food concentration<sup>93</sup> (see also Chapters 8 and 9 for further discussion of the effects of temperature on metabolism).

### *Potential impact and adaptive capacity*

The potential impact of the projected temperature increases on the food webs for tuna in all provinces, particularly under the A2 scenario in 2100, will depend on the capacity of the organisms to adapt to any temperatures beyond those they presently encounter. The  $Q_{10}$  index outlined above also describes the capacity of organisms to adapt to increases in temperature over a certain range; it is  $\sim 2$  for adapted organisms and  $< 2$  or  $> 2$  for those species that are unable to control the effects of temperature increase<sup>92</sup>. Both cyanobacteria<sup>91</sup> and copepods<sup>92</sup> have adapted to the temperature range occurring in the region, which commonly includes temperatures of 31–32°C in the Warm Pool.

### *Vulnerability*

The organisms that comprise the food webs for tuna are already exposed to high temperatures in all provinces and appear to have a low vulnerability to the projected effects of increases in water temperature under the B1 and A2 scenarios for 2035 and 2100. However, vulnerability is expected to vary among this wide range of organisms due to their individual adaptive capacities.

## 4.8.2 Mixed layer depth

### *Exposure and sensitivity*

The maximum depth of the mixed layer is projected to be shallower under climate change in all provinces, especially in PEQD. This ‘shoaling’ is expected to be most pronounced under the A2 scenario in 2100 (Section 4.7, Chapter 3). Since the projected shoaling will be accompanied by a greater temperature (and density) gradient, nutrient supply from deeper layers by eddy diffusion and mixing will be reduced as in Cases 1 and 2 (Figure 4.3). Shoaling of the MLD to an extent that is similar to that projected under climate change presently occurs in the gyres in summer and reduces the availability of nutrients in these areas during this season. In the Warm Pool, the transfer of nutrients to the mixed layer is of less significance than in the gyres because the thermal gradient is always strong in this province and the key factor is the MLD compared with the depth of the photic zone. As discussed before (Case 1, Figure 4.3), when the MLD is deep, NPP is reduced in the Warm Pool. Conversely, a shoaling of MLD will increase NPP by providing more light to the nutrient-rich photic zone below the MLD (Case 2, Figure 4.3). Food webs are sensitive to the changes that presently occur in the MLD between summer and winter in the two gyres, and with ENSO in the Warm Pool.



Zooplankton: postlarval crab ~ 1 cm (left) and copepod < 1 mm (right)

Photos: Anita Slotwinski

### *Potential impact and adaptive capacity*

The increase in oligotrophic conditions associated with the projected changes to the mixed layer within the photic zones of the gyres is expected to reduce the biomass of phytoplankton, and increase the proportion of phytoplankton of a small size (Section 4.2.1). In turn, the smaller phytoplankton cells are expected to increase the proportion of small-sized herbivores and carnivores, leading to a greater number of trophic links between phytoplankton and tuna at the top of the food web. In other words, the food web in these provinces is likely to become less efficient and, therefore, poorer as the supply of new nutrients is reduced.

There is little capacity for maintaining existing proportions of larger-sized phytoplankton in the food webs in the gyres if conditions become more oligotrophic. Many of the common species of phytoplankton are unlikely to be able to adapt to more oligotrophic conditions. Instead, they are expected to be replaced by other species.

### *Vulnerability*

Food webs in NPTG, SPSG and the Warm Pool under normal and La Niña conditions have a moderate to high vulnerability to changes in the depth of the mixed layer. In the gyres, a shallower MLD with a strong density gradient, as occurs presently in summer, will lead to a less productive ecosystem. Such a situation, if it persists all year, would result in reduced food for tuna in the gyres. In the Warm Pool, a deeper MLD would lead to a less productive ecosystem, as happens presently during La Niña events. The extent of such vulnerability depends on the effects of global warming on the existing seasonal patterns in the gyres, and the interannual patterns in the Warm Pool in relation to the MLD.

## **4.8.3 Upwelling**

### *Exposure and sensitivity*

Upwellings do not occur in the Warm Pool or the gyres. In ARCH, they occur on a limited scale on a temporary basis. Therefore, exposure of food webs to any changes in upwelling of nutrient-rich water is expected to occur mainly in PEQD. Primary productivity in PEQD is limited by iron (Section 4.3.1), so exposure to changes in iron concentrations also needs to be considered here.

No major changes are expected in upwelling in PEQD under the B1 and A2 scenarios (Chapter 3). However, because iron originates mainly from the Equatorial Undercurrent (EUC), exposure to iron concentrations in PEQD may increase. This is likely to occur because the EUC is projected to increase in strength over the 21<sup>st</sup> century, and move progressively upwards, by about 10 m under B1 and A2 in 2035 and B1 in 2100, and then by 20 m for A2 in 2100 (Chapter 3). Aeolian inputs of

iron to PEQD are negligible at present but this could change with variations in the location of the Intertropical Convergence Zone (ITCZ) (Chapter 2).

The food web in PEQD has a low sensitivity to any changes in macronutrients (Section 4.3.1), except for silicate, which needs to be above a certain concentration for diatoms to grow<sup>11</sup>. However, provided the supply of nutrients is maintained close to its current level, this food web is highly sensitive to any change in iron concentrations.

#### *Potential impact and adaptive capacity*

As long as equatorial upwelling remains strong, the supply of macronutrients is unlikely to limit primary production in PEQD. The IronEx experiments (Section 4.5) demonstrate how equatorial phytoplankton are limited by iron concentrations. Therefore, increases in iron, derived from projected changes to the EUC, create the potential for increased primary production and greater proportions of large-sized phytoplankton in PEQD (Section 4.2.1). The potential impact of higher concentrations of iron would be a food web for tuna with fewer links, leading to a larger biomass of top predators.

#### *Vulnerability*

Food webs for tuna in PEQD are expected to have a low positive response to projected increases in upwelling and increased iron concentrations. Whether these benefits materialise will depend on the interactions between the intensity of upwelling and the velocity of the EUC.

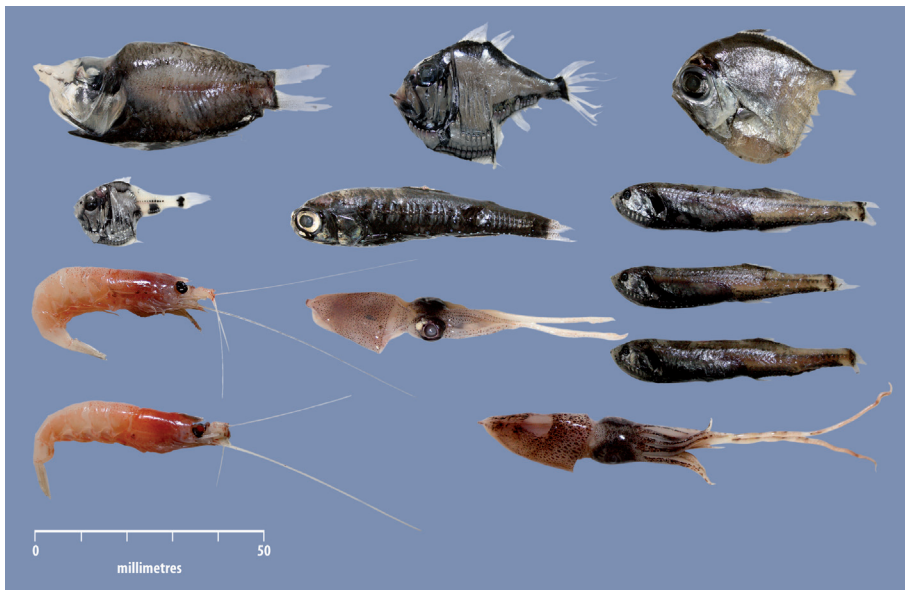
### **4.8.4 Solar and ultraviolet radiation**

#### *Exposure and sensitivity*

The Warm Pool and much of ARCH (except New Caledonia) are projected to have increased levels of cloud cover in the area of the South Pacific Convergence Zone (SPCZ) associated with the higher levels of rainfall expected to occur there as a result of global warming (Chapter 2). Similar conditions are also expected to eventuate for PEQD around the ITCZ. The projected increases in rainfall are within the range of 5–20% for the B1 and A2 scenarios by 2035, and 10–20% for B1 and A2 by 2100. However, reduced cloud cover is expected for subtropical parts of SPSG and NPTG, where rainfall is expected to decline by 5–20% by 2100 (Chapter 2).

Primary production is sensitive to light in two main ways. First, photosynthesis is reduced in the upper water column due to photo-inhibition, with the result that photosynthesis is usually at its maximum at a depth of 30 m in PEQD (Figure 4.7), where macronutrient concentrations do not limit the growth of phytoplankton. In contrast, photosynthesis is at a maximum at a greater depth in the oligotrophic provinces due to nutrient limitation, not photo-inhibition. Second, photosynthesis

is lower during overcast days and total primary production throughout the water column can be reduced 1.5 to 3 times when surface light intensity is only 10% of that on a sunny day. Differential susceptibility of microbes to ultraviolet radiation (UVR) is potentially an important determinant of community structure of both bacteria<sup>94</sup> and photosynthetic picoplankton<sup>95</sup>. Because phytoplankton are sensitive to UVR, increased UV-B can result in a decrease in photosynthesis<sup>96</sup>. The effects of changes in UVR are ameliorated by vertical mixing and by the production of UV-absorbing compounds and antioxidants. UVR has also been shown to reduce copepod survival and fecundity<sup>97</sup>.



Typical micronekton in the diet of tropical Pacific tuna

Photo: Jean-Pierre Lebars

### *Potential impact and adaptive capacity*

Increased cloud cover is expected to have limited impact on total primary production of the water column in the Warm Pool, ARCH and PEQD. In the gyres, no change is expected due to reduced light, because the vertical distribution of nutrients is the key factor controlling primary productivity. In SPSSG, however, greater light intensity and UVR are expected to increase photo-inhibition on more days in the upper 10 m of the water column. However, this is expected to have little impact because only a small part of total primary production typically takes place in this layer in oligotrophic provinces. Zooplankton living at the surface in SPSSG are adapted to natural light intensities and should not suffer from extra UVR. Indeed, many zooplankton are adapted to a certain range of light intensities and wavelengths, and migrate to depths where they find their optimal light characteristics<sup>97</sup>.

### *Vulnerability*

All parts of the food web are expected to have a very low vulnerability to changes in solar radiation. Nevertheless, alterations in availability of light have the potential to change the structure of the picoplanktonic community in surface waters (down to a

depth of 10 m), causing a shift from photosynthetic picoplankton to bacterioplankton, because of their different susceptibilities (see above). However, only a small fraction of the total phytoplankton biomass occurs in the upper layer of oligotrophic provinces, and mixing of the surface layer in all provinces prevents planktonic organisms from staying in the upper part of the photic zone for long. Overall, therefore, changes in the flux of solar radiation on the surface of NPTG and SPSG are expected to have a very weak impact on primary production.

#### 4.8.5 Dissolved oxygen

##### *Exposure and sensitivity*

In the tropical Pacific Ocean, average concentrations of O<sub>2</sub> at a depth of 300 m are projected to decrease by 0.2 ml per litre by 2100 under the A2 scenario (Chapter 3) (minimum concentrations of O<sub>2</sub> throughout the water column usually occur at this depth). By 2100, O<sub>2</sub> concentrations in the provinces themselves are expected to decline by < 5% at 300 m in most cases, except for NPTG, where they could increase by up to 8%, and PEQD, where they would be 5–26% lower (Table 4.3). It is important to note that the projected decreases do not apply to the photic layer, which is largely in equilibrium with atmospheric O<sub>2</sub>. Rather, the decreases are expected to be due to oceanic processes occurring at higher latitudes, which result in lower concentrations of O<sub>2</sub> in deeper water in the tropics (Chapter 3).

The food web in deep waters (to a depth of 1000 m) is comprised of organisms which require O<sub>2</sub> to break down organic substrates, such as carbohydrates, and release the products through respiration and excretion. This catabolic process produces energy which is used for locomotion, growth and reproduction. Therefore, many of the organisms in the food web for tuna cannot live in anoxic (no oxygen) conditions for long periods. Some species living below the photic zone, however, e.g. bathypelagic copepods, can tolerate hypoxic conditions (low O<sub>2</sub> concentration)<sup>92,98</sup>. In such situations, these organisms have a decreased respiration rate.

##### *Potential impact and adaptive capacity*

In all provinces, except NPTG, the projected decrease in dissolved oxygen is unlikely to have a damaging effect on the food webs for tuna – concentrations of O<sub>2</sub> there are already relatively high (Table 4.3) and decreases of < 5% are not expected to affect these organisms. Furthermore, in the event of any localised, more severe, depletions of O<sub>2</sub>, macrozooplankton and micronekton that undergo diurnal vertical migrations can escape anoxia by moving to more oxygenated areas within the water column. However, a possible consequence of such movement can be ‘compression’ of the feeding habitat for tuna, leading to greater rates of predation. Depending on where these feeding areas occur, tuna may be more vulnerable to surface fisheries<sup>99</sup> (Chapter 8). Other components of the food web, e.g. micronektonic fish, are usually ‘non-migrants’ and, although some of these species can tolerate anoxic conditions, other species cannot<sup>100,101</sup>.



Zooplankton in the food web for tuna

Photo: Photoshot/SuperStock

### *Vulnerability*

Projected changes in O<sub>2</sub> concentrations at a depth of 300 m are thought to be generally too low to cause significant changes in the food webs that support tuna.

## **4.8.6 Ocean acidification**

### *Exposure and sensitivity*

Due to the decrease in pH arising from the increased concentration of CO<sub>2</sub> in the ocean, average aragonite (one of the two forms of calcium carbonate) saturation in surface waters is projected to decline from the present value of 3.9 (350% saturation) to around 3.0 for the B1 scenario by 2100, and to 2.4 for A2 by 2100 across the region (Chapter 3).

Projections for the various provinces show a similar but less pronounced trend in  $\Omega$  aragonite (Section 4.7.2, Table 4.3). These decreases can be converted into declines of 2–9% in calcification rates for organisms like pteropods (pelagic molluscs), which means the projected effects of acidification across the tropical Pacific Ocean are low compared with those for the Southern Ocean<sup>102</sup>. Although these declines are expected to be greatest near the surface, the depth of the aragonite saturation horizon (below which aragonite dissolves) is also expected to decrease to within 150 m of the surface in 2100 under the A2 emissions scenario at 8°N, and to a lesser extent to the north and to the south (Chapter 3).

As described in Section 4.5, some organisms in the food web for tuna, e.g. pteropod molluscs, depend on the present-day supersaturation state for aragonite to build robust shells and skeletons<sup>79</sup>. These organisms will need to expend more energy to form aragonite as the saturation horizon for aragonite becomes shallower, and supersaturation levels in the surface waters decrease<sup>103</sup>. Other organisms, such as coccolithophorids (haptophytes) in the phytoplankton, and foraminiferans and non-pteropod molluscs in the zooplankton, have shells made of calcite. They are expected to be less sensitive because greater decreases in pH are needed for 'shoaling' of the calcite saturation horizon<sup>102</sup>.

### *Potential impact and adaptive capacity*

Ocean acidification is expected to reduce the shells of calcareous phytoplankton and zooplankton, making them more fragile and vulnerable to predation. Some of these organisms may eventually disappear, causing changes in the complexity of food webs. For example, the pteropods that feed on very small particles ( $< 1 \mu\text{m}$  diameter), might be replaced by tunicates. Since tunicates have very short life spans, the altered grazing pressure and response to variation in picophytoplankton abundance may lead to food webs that function differently. Foraminiferans might also be replaced by silicic radiolarians, which feed in a similar way, thus reducing the concentrations of silicate. Because silicate is vital for diatoms, acidification may have an indirect effect on the species composition of phytoplankton.

Although ocean acidification could have unpredictable and cascading effects on food webs, the calcareous organisms likely to be affected directly are a minor part of the ecosystem. In PEQD, for example, they represent only 1–5% of the phytoplankton<sup>104</sup>, 6.1% of the microzooplankton and mesozooplankton<sup>105</sup> and 2.2% of the micronekton<sup>22</sup>. Similar proportions apply to the other provinces. On the other hand, the loss of the calcareous organisms could have a dramatic effect on the transfer of anthropogenic carbon from the photic zone to the deep ocean via the process known as the 'biological carbon sink'<sup>106</sup>.

### *Vulnerability*

Organisms living in the upper part of the tropical Pacific Ocean are likely to have low vulnerability to the projected changes in ocean acidification. Calcifying animals living at some greater depths would be more vulnerable due to the reduced depth of the aragonite saturation horizon. However, because of the small contribution of calcareous organisms to micronekton, the impact of acidification on tuna forage should be small.

## 4.9 Integrated vulnerability assessment

The biogeochemical modelling (Section 4.7) integrated the effects of the projected changes to the physical and chemical features of the ocean on the supply of nutrients, NPP and the biomass of zooplankton in each province. The projected changes in NPP and zooplankton biomass are shown in Figures 4.14 and 4.15, respectively, and in Table 4.3.

To assess the vulnerability of food webs for tuna in each province, these projected changes also need to be integrated with expected alterations in the surface area of each province (Figure 4.13, Table 4.3). The main projections resulting from the integration of all the factors above are summarised for each province below.

### 4.9.1 Integrated assessments for each province

The food web in PEQD is expected to have a moderate vulnerability to the increases in greenhouse gas emissions in 2035, and a high vulnerability by 2100 (Table 4.3). This is due mainly to substantial decreases (20–50%) in the size of this important province (Table 4.3), and its relocation further east (Figure 4.13). Changes to NPP and the biomass of zooplankton in the food webs for tuna themselves within the more limited PEQD are expected to be slight (Table 4.3). The possible implications for tuna include an overall reduction in the quantity of forage previously available in PEQD, and relocation of the main feeding area for tuna (the convergence zone between PEQD and the Warm Pool – see Chapter 8) further to the east. Similar changes already occur regularly due to El Niño events, and the effects of projected changes to PEQD can be expected to mimic those due to ENSO closely (Chapter 8).

The food web in the Warm Pool is also expected to have a moderate vulnerability under the B1 and A2 scenarios in 2035, and a high vulnerability in 2100 (Table 4.4). Once again, this is driven mainly by the substantial projected changes to its surface area (Figure 4.13, Table 4.3), which resemble the effects of El Niño on this province. However, an important difference is that whereas the nutricline in the Warm Pool becomes shallower during El Niño episodes and increases nutrient supply to the photic zone and NPP, the projections under global warming show a deepening of the nutricline. Such deepening is expected to lead to reductions of up to ~ 10% in NPP (integrated throughout the water column) and zooplankton biomass by 2100 in the Warm Pool (Table 4.3).

The projected reduction in NPP in the Warm Pool is a possible threat to the production of tuna because it presents a markedly different situation than the one that presently appears to operate towards the end of an El Niño event, when the increased NPP from a shoaling of the nutricline appears to trigger the movement of tuna westwards<sup>5</sup>.

Taken together, the projected reduction in the area of PEQD, and the expansion of the nutrient-poor Warm Pool, will result in a more oligotrophic equatorial Pacific Ocean.

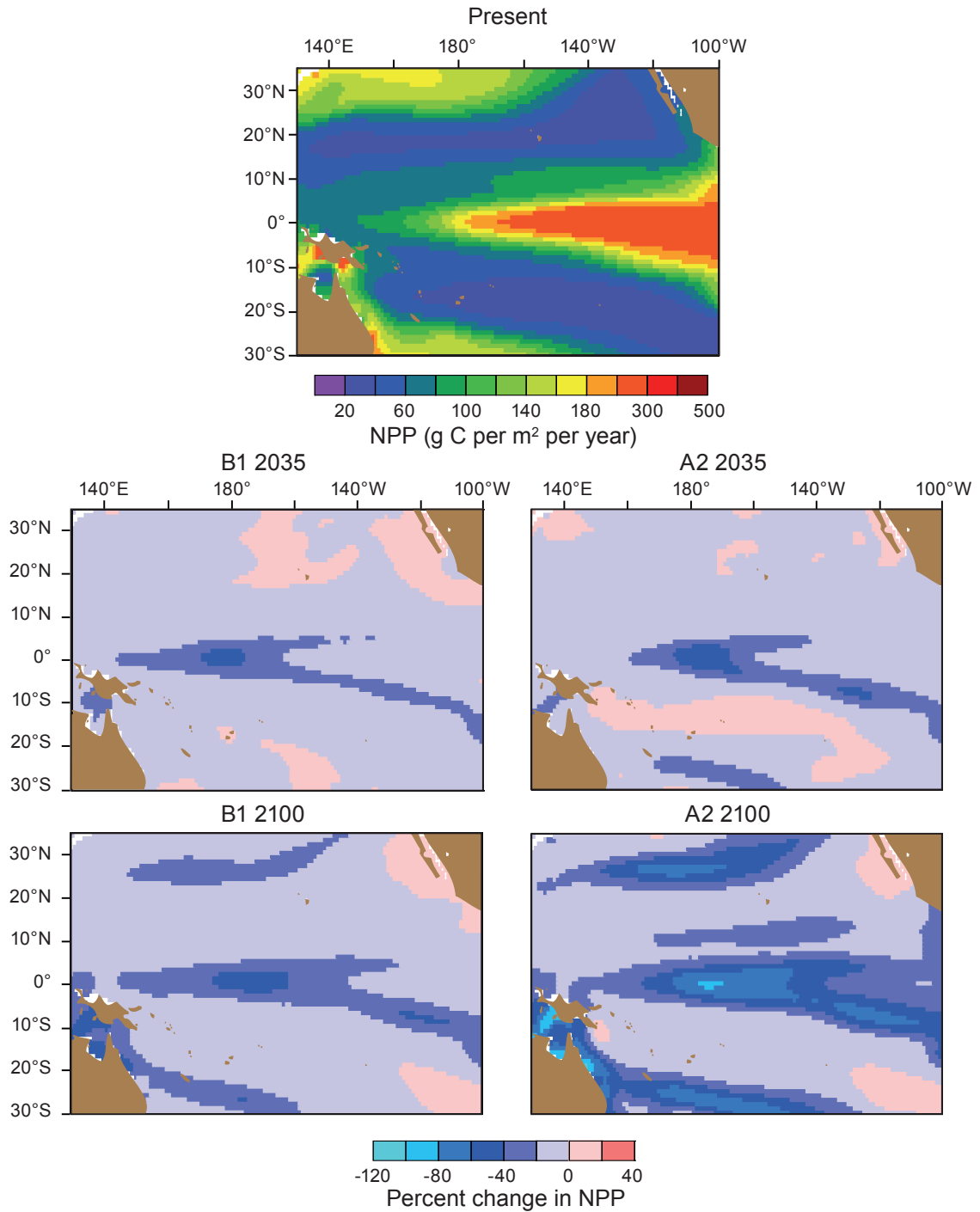


**Figure 4.14** Present-day net primary production (NPP) across the tropical Pacific Ocean and projected percentage changes in NPP under the B1 and A2 emissions scenarios for 2035 and 2100, relative to present conditions.

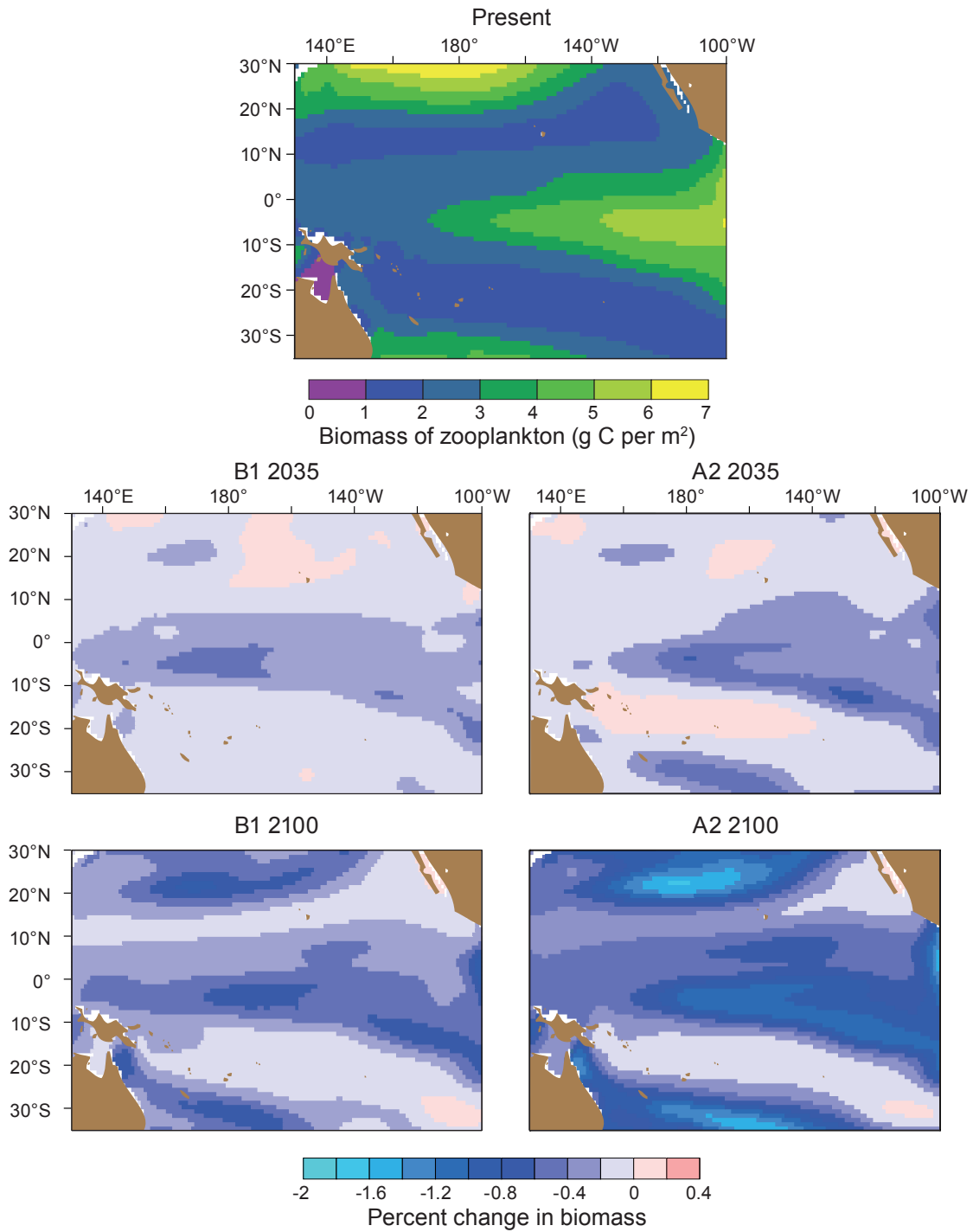


**Figure 4.15** Present-day biomass of zooplankton across the tropical Pacific Ocean and projected percentage change in this biomass under the B1 and A2 emissions scenarios for 2035 and 2100, relative to present conditions.

The food web in SPSG is expected to have a low vulnerability in 2035 due to the limited expansion in area and decreased NPP and zooplankton biomass projected to occur by that time (Table 4.4). However, continuation of these trends will result in the vulnerability increasing to low-moderate by 2100 (Tables 4.3 and 4.4). The vulnerability of the food webs in NPTG is considered to be low in 2035 (Table 4.4) due to negligible changes in surface area and only modest changes in NPP and zooplankton biomass. However, vulnerability is expected to be moderate by 2100 under both the B1 and A2 scenarios because NPP is projected to decrease by 11–22% and the biomass of zooplankton is expected to decline by 10–18% (Table 4.3). In both gyres, the biogeochemical modelling indicates that the projected decreases in NPP and zooplankton biomass are expected to be concentrated at the poleward extremes of these provinces.

In ARCH, the main effects of global warming are projected to decrease the availability of nutrients through variations in the depth of the mixed layer (Table 4.3) and the incursion of more oligotrophic water from SPSG. As a result of these limited changes, the food web for tuna in ARCH is expected to have a low vulnerability in 2035 under both the B1 and A2 emissions scenarios (Table 4.4). By 2100, ARCH is expected to have a moderate vulnerability because NPP and the biomass of zooplankton are projected to decline by 20–33%, and 17–26%, respectively (Table 4.3) due to greater expansion of nutrient-poor water from SPSG. Note, however, that the magnitude of the decline in ARCH may be questioned because simulations with another global climate model (CSIRO model) indicate that much smaller changes are expected<sup>107</sup>.

#### 4.9.2 Ecopath model for the Warm Pool

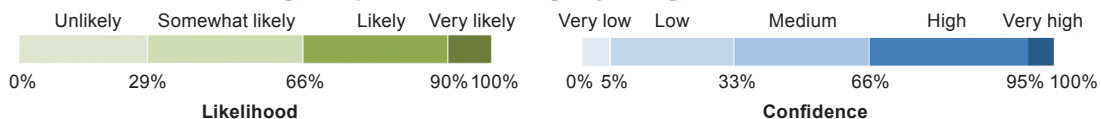
To examine the effects of projected changes to NPP in the Warm Pool in 2035 and 2100 on the food web for tuna, and on the expected catches of tuna from the province, we used ‘Ecopath with Ecosim’, a trophic mass-balance ecosystem model<sup>108,109</sup>. Ecopath describes the static state of energy flows in a food web that balances the net production of a group with all sources of mortality and migration<sup>110</sup>. Ecosim re-expresses the static Ecopath model in a dynamic form, whereby the dynamics and sensitivity of the model are controlled largely by the predator consumption rates and the proportion of the prey vulnerable to predation.

Ecopath and Ecosim simulations help test the effects of fishing and environmental change scenarios by forcing variations in biomass on selected components of the ecosystem<sup>111,112</sup>. However, Ecopath and Ecosim are sensitive to the relative strengths of indirect and direct physical effects on middle and upper trophic levels. Another important limitation of these models is the absence of direct links with physical oceanography and nutrients.

**Table 4.4** Integrated vulnerability assessments (across all variables described in Section 4.8) for each of the five ecological provinces in the tropical Pacific Ocean for 2035 and 2100 for the B1 and A2 scenarios combined. Where ranges of values are provided for the projected changes, the lower and higher values represent the projections for B1 and A2, respectively. The likelihood and confidence values associated with these assessments are also shown.

| Province  | Year | Vulnerability    | Projected changes  |
|-----------|------|------------------|--|
| PEQD      | 2035 | Moderate<br>     | Decrease in surface area of 20–27% as western boundary of PEQD moves eastwards from 180° to 170°W. Minor (2%) reduction in zooplankton biomass. No direct effect of higher SST, and lower O <sub>2</sub> and pH, on biomass or composition of plankton.                              |
|           | 2100 | High<br>         | Decreases in surface area of 30–50% and movement of boundary to 160–150°W. A 2–4% increase in NPP and 3–6% decrease in biomass of zooplankton. No direct effect of higher SST, and lower O <sub>2</sub> and pH, on biomass or species composition of plankton.                       |
| Warm Pool | 2035 | Moderate<br>     | Increase in surface area eastwards by 18–21%, with a 5–7% reduction in NPP and 3–6% decrease in biomass of zooplankton throughout the water column. No direct effect of higher SST, and lower O <sub>2</sub> and pH, on biomass or species composition of plankton.                  |
|           | 2100 | High<br>         | Increase in surface area eastwards by 26–48%, with a 9% reduction in NPP and 9–10% decrease in biomass of zooplankton throughout the water column. No direct effect of higher SST, and lower O <sub>2</sub> and pH, on biomass or species composition of plankton.                   |
| NPTG      | 2035 | Low<br>          | Surface area increases limited to 1% as the province extends to the north. NPP decreases by 3–5% and zooplankton biomass declines by 3 to 4%. No direct effect of higher SST and O <sub>2</sub> , or lower pH, on biomass or species composition of plankton.                        |
|           | 2100 | Moderate<br>     | Increase in surface area stabilises at an increase of 1% but NPP decreases greatly (11–22%) and biomass of zooplankton declines by 10–18%. No direct effect of higher SST and O <sub>2</sub> , or lower pH, on biomass or species composition of plankton.                           |
| SPSG      | 2035 | Low<br>          | Surface area increases by 3–7%. NPP decreases by 4–5% and biomass of zooplankton declines by 3–4%. No direct effect of higher SST, and lower O <sub>2</sub> and pH, on biomass or species composition of plankton.   |
|           | 2100 | Low-Moderate<br> | Surface area increases by 7–14% and extends poleward, with a 3–6% reduction in NPP and 5–10% decrease in biomass of zooplankton due to deepening of the thermocline. No direct effect of higher SST, and lower O <sub>2</sub> and pH, on biomass or species composition of plankton. |
| ARCH      | 2035 | Low<br>          | No change in surface area. A reduction in NPP of 5–8% and a 5–6% decrease in biomass of zooplankton due to deepening of the thermocline. No direct effect of higher SST, and lower O <sub>2</sub> and pH, on biomass or species composition of plankton.                             |
|           | 2100 | Moderate<br>     | No change in surface area. Greater (20–33%) reduction in NPP and a 17–26% decrease in biomass of zooplankton due to deepening of the thermocline. No direct effect of higher SST, and lower O <sub>2</sub> and pH, on biomass or species composition of plankton.                    |

SST = sea surface temperature; O<sub>2</sub> = dissolved oxygen percentage saturation at 300 m; PEQD = Pacific Equatorial Divergence; Warm Pool = Western Pacific Warm Pool; NPTG = North Pacific Tropical Gyre; SPSG = South Pacific Subtropical Gyre; ARCH = Archipelagic Deep Basins.



For the purposes of this analysis, we defined the Warm Pool as the area 10°N–15°S and 110°E–165°E. The biota described from the Warm Pool were assigned to one of 44 functional groups (including detritus and fishery discards) based on their ecological similarity, feeding mode, diet, size, and rates of production and consumption. The model simulations were run until 2035 and 2100, relative to 2000–2010, using 2005 as the starting point. Changes in the biomass of mesozooplankton, epipelagic micronekton, mesopelagic micronekton and bathypelagic micronekton were simulated by introducing linear decreases in the biomass of small and large phytoplankton of 6% by 2035 and 9% by 2100, projected by the IPSL/PISCES model (Table 4.3). While projections on Table 4.3 refer to NPP, they can be considered to represent phytoplankton biomass because NPP approximates biomass on a daily basis in the steady-state ecosystems of the tropical Pacific Ocean. The model also simulated the effects of reductions in phytoplankton at the base of the food web on the catches of adult skipjack, yellowfin and bigeye tuna from the Warm Pool in 2035 and 2100. Note that the projected decreases in NPP and, consequently, phytoplankton biomass in 2035 and 2100 are comparable for the B1 and A2 emissions scenarios (Table 4.3).

The diet matrix for the functional groups was based on stomach content analyses undertaken by the SPC Oceanic Fisheries Programme and supplemented by other research in Australia and PNG<sup>28,113,114</sup>. Estimates of forage biomass were obtained from the SEAPODYM model<sup>115</sup> (Chapter 8). The key biological parameters (biomass, production/biomass ratio, consumption/biomass ratio, ecotrophic efficiency, diet composition and catch) for each functional group were derived from primary research data, stock assessments, fishery data recorded in logbooks or by scientific observers, or the literature.

To increase the reliability of projections from Ecosim, the model was fitted to time-series of biomass, fishing mortality and catch data for twelve functional groups of predatory fish: juvenile bigeye tuna (ages 0–4 years), adult bigeye tuna (5–10 years), small juvenile skipjack (0–4 months), juvenile skipjack (5–12 months), large skipjack (1–4 years), juvenile yellowfin tuna (0–2.25 years), adult yellowfin tuna (2.5–7 years), striped marlin (1–10 years), South Pacific albacore (1–5 years) and blue marlin (0–21 years), juvenile swordfish (1–2 years), and adult swordfish (3–20 years). These data were derived from spatially-explicit, age-structured stock assessment models for the period 1952–2008<sup>116–119</sup>.

The projected reductions of phytoplankton of 6% in 2035 caused approximately proportional decreases in the projected biomass of mesozooplankton and epipelagic micronekton (Figure 4.16a). Even greater decreases in the biomass of mesopelagic and bathypelagic micronekton are projected by the model (Figure 4.16a). This is primarily due to the production/biomass ratios for mesopelagic and bathypelagic groups being less than half that of the mesozooplankton and epipelagic micronekton group. In other words, the former groups have a lower capacity to recover after biomass declines due to climate change.

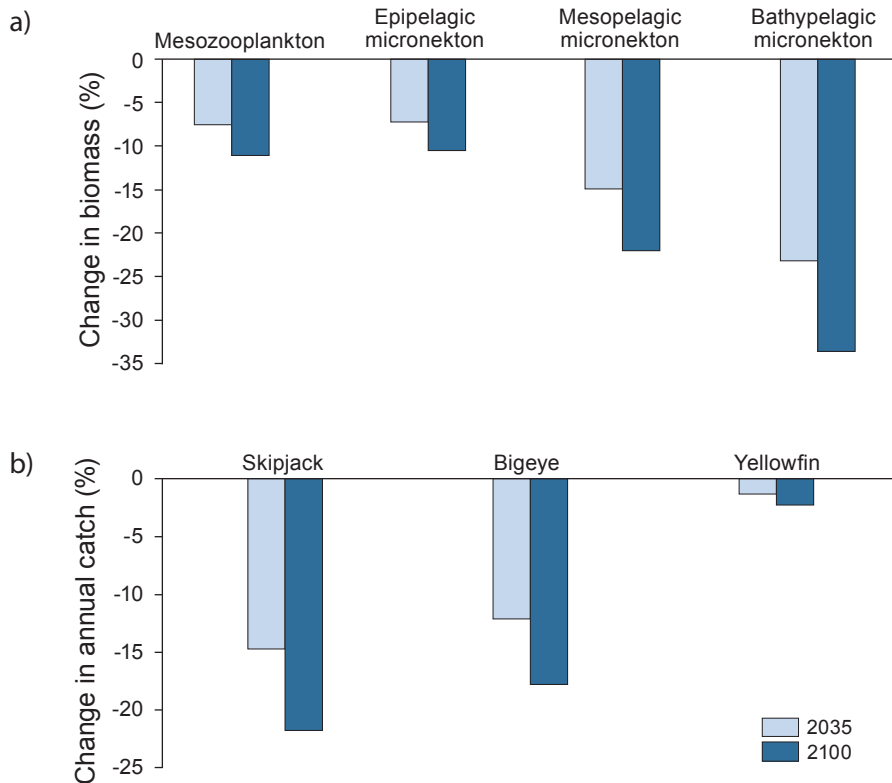


**Figure 4.16** Changes in (a) the biomass of mesozooplankton and the various types of micronekton in the food web for tuna; and (b) the catches of the main tuna species, in the Warm Pool in 2035 and 2100 relative to 2000–2010, projected by the Ecopath model.

The expected changes in mesozooplankton and micronekton are projected to have the greatest effect on skipjack tuna, with the simulations indicating that catches of this species in the Warm Pool could fall by ~ 15% in 2035 (Figure 4.16b). These projected effects are due to the higher biomass of epipelagic micronekton, compared with mesopelagic and bathypelagic micronekton, and the relative importance of epipelagic micronekton in the diet of skipjack tuna. Significant decreases in catches of bigeye tuna are also projected in 2035, but the effects on the catches of yellowfin tuna are projected to be minor (Figure 4.16b). Yellowfin tuna are projected to be less affected for two reasons. First, they have a higher production/biomass ratio, which allows the species to have a greater capacity to withstand changes in their biomass due to external factors. Second, the more diverse diet of yellowfin tuna enables them to shift their feeding preferences towards more abundant taxa in their forage arena, which are less affected by climate change.

The projected 9% decrease in biomass of phytoplankton in 2100 results in proportionally higher declines in the biomass of mesozooplankton and micronekton, and catches of tuna (Figure 4.16).

Caution is needed in interpreting the projections of ecosystem-level response to climate change in the Warm Pool Ecopath model. Ecopath does not directly integrate all effects of climate, such as changes in animal movements induced by temperature changes, mixed layer depth variations and oxygen minimum layer depths. Instead, the model primarily relies on external models to be able to predict the effects of climate change on biomass of specific groups (e.g. phytoplankton), which can be used to 'drive' the model.

These features of Ecopath help to explain the differences between the projected catch rates for skipjack made here and those made using the SEAPODYM model in Chapter 8. By driving the model using biomass of phytoplankton, we implicitly assume that the food web is controlled by bottom-up processes. Yet an increasing number of models for pelagic ecosystems worldwide indicate that oceanic food webs have a more complex 'wasp-waist' structure, where the majority of the biomass is comprised of mid-trophic level groups. These groups are critical to the maintenance of ecosystem structure because they function as important predators of zooplankton and are prey of high-trophic level predators, such as tuna. For example, a recent model of the pelagic ecosystem off eastern Australia demonstrated the importance of mid-trophic level mesopelagic fish and cephalopods (micronekton) for exerting top-down control on lower trophic levels, and bottom-up control on these levels as prey for large tuna, billfish and sharks<sup>120</sup>. The inference is that any significant alteration in the biomass of micronekton due to the processes described in this chapter may cause large and unpredictable changes to the biomass of higher and lower trophic levels, and the overall integrity of the ecosystem.

#### **4.10 Uncertainty, gaps in knowledge and future research**

Although the modelling described here indicates strongly that changes could occur in the food webs for tuna in some provinces, there is much uncertainty associated with these projections. The uncertainty arises because even though oceanographic science has made huge progress during the last 40 years, the projections are based on rather scant knowledge of natural variability in the dynamics of phytoplankton and zooplankton populations.

In the tropical Pacific Ocean, the only information on long-term changes in abundance of phytoplankton and zooplankton comes from the HOT station in NPTG. Although the 24-year dataset from HOT has documented interannual and decadal variability, the record is not yet long enough to show any trend which could be linked to climate change. The imperative is to establish similar comprehensive monitoring programmes in the other provinces, particularly PEQD and the Warm Pool. The Tropical Atmosphere Ocean (TAO) array of moorings deployed by NOAA between 8°S and 8°N from 1984 to 1994, which are still operating with support from Japan and France provide a basis for a monitoring programme in PEQD and the Warm

Pool. However, biochemical sensors will need to be added to the existing capability, which measures meteorological and hydrographical parameters, and in a few cases, currents, nutrients and chlorophyll *a*.

Ideally, acoustic devices should also be installed among such arrays to monitor zooplankton and micronekton. However, acoustic data still suffer from poor correlations with micronekton sampled with nets, and the species composition and relative abundance of micronekton from stomach contents of tuna and other top predators<sup>69,121,122</sup>. To validate acoustic data, we need reliable information on spatial and temporal variation in the species composition and relative abundance of micronekton. Increasing the reliability of the acoustic data would also open the way for fitting suitable instrumentation to 'ships of opportunity', to build up time-series along the major shipping routes in the region.

A continuous remote sensing record of ocean colour, linked to chlorophyll *a* and other pigments, has been available for all provinces since the inception of the US Sea WiFS (Wide Field-of-View Sensor) mission in September 1997, and from other satellites launched later. With appropriate corrections (e.g. for nebulosity) applied to satellite images, remote sensing is being used to document phytoplankton biomass in the superficial layer of the ocean, down to a depth of 20 m in oligotrophic provinces. The focus is on identifying the relationships between concentrations of chlorophyll *a* in the surface and deep layers. This varies with the type of ecosystem being considered, so the relationship in the Warm Pool, for example, is expected to be different to that for the gyres.

Three key information gaps need to be filled by monitoring programmes to parameterise future models in a better way.

- Spatial and temporal distribution of iron in the EUC, and the bio-availability of the different forms of iron.
- Variability in abundance of micronekton, and the factors driving this variability, including production processes taking place in the photic zone, the complexities of food webs, and the differential life spans of the prey species and their predators.
- Lateral transport of organisms within and between provinces, as described for PEQD<sup>39,123</sup>. Such processes are poorly understood but have been implicated in the transfer of organic matter from rich oceanic zones to poorer ones in the equatorial Pacific<sup>124</sup>. We particularly need to know the extent of exchanges between provinces within the aphotic zone.

The resolution of models also needs to be improved substantially to reduce uncertainty. At present, the coupled atmosphere ocean model used to simulate oligotrophic regions lacks eddies, which are an important mechanism for transferring nutrients into the photic zone (Chapter 3). The current generation of ocean models underestimate NPP, resulting in considerable uncertainty in projecting the effects of

climate change on this vital process. In particular, there are several features of the present climate used by the IPSL model that influence the simulated decline in NPP with climate change. For example, the modelled position of the SPCZ in the Southern Hemisphere is too far north, and high productivity occurs along the entire east coast of Australia. This makes the averaged NPP in ARCH and SPSG too great.

At present, modelling the effects on micronekton has only been done using Ecopath with Ecosim for the Warm Pool (Section 4.9.2). Much care is also needed in using these tools to simulate cascading effects of trophic interactions within provinces. Although this suite of models can make trophic links between the different components of the ecosystem, there are no direct connections to physical models. Instead, climate change scenarios are usually simulated in Ecosim by imposing variations in biomass of various components (e.g. phytoplankton biomass).

The uncertainties and gaps in knowledge lead us to conclude that the changes projected to occur by coupled models in the provinces need to be interpreted with caution. Given the great importance of PEQD, it is essential that the confidence for modelling the response of this rich province to climate change is improved. Provided models are able to accurately project the surface areas of PEQD and the Warm Pool, impacts on both ecosystems can be inferred from known ENSO-related changes. The great reductions of PEQD during the two strong El Niño events between 1980 and 2000<sup>30</sup> are examples of such ENSO-related changes.

#### 4.11 Management implications and recommendations

The sheer size of the provinces in the tropical Pacific Ocean makes it extremely difficult to think of any management interventions that could be applied at a meaningful scale. The relatively low concentrations of iron required to increase primary production in PEQD means that iron fertilisation is potentially one such possibility. However, caution is needed because the long-term biogeochemical<sup>125</sup> and ecological effects of iron enrichments are still largely unknown. The code of practice for such geoengineering research specified under the London Convention and Protocol<sup>ii</sup> needs to be applied in any future investigations to improve iron concentrations in PEQD. The single greatest intervention to reduce the effects of climate change on the provinces identified here is global reduction of greenhouse gas emissions.

ii [www.londonprotocol.imo.org](http://www.londonprotocol.imo.org)

## References

1. Longhurst AR (2006) *Ecological Geography of the Sea*. Academic Press, New York, United States of America.
2. Pomeroy LR (1979) Secondary production mechanisms of continental shelf communities. In: RJ Livingstone (ed) *Ecological Processes in Coastal and Marine Systems*. Plenum Press, New York, United States of America, pp. 163–186.
3. Longhurst AR (1991) Role of the marine biosphere in the global carbon cycle. *Limnology and Oceanography* 36, 1507–1526.
4. Fasham MJR (2003) *Ocean Biogeochemistry. The Role of the Ocean Carbon Cycle in Global Change*. Springer Verlag, Berlin, Germany.
5. Lehodey P, André JM, Bertignac M, Hampton J and others (1998) Predicting skipjack tuna forage distributions in the equatorial Pacific using a coupled dynamical biogeochemical model. *Fisheries Oceanography* 7, 317–325.
6. Lehodey P, Chai F and Hampton J (2003) Modelling climate-related variability of tuna populations from a coupled ocean-biogeochemical-populations dynamics model. *Fisheries Oceanography* 12, 483–494.
7. Friedlingstein P, Cox P, Betts R, Bopp L and others (2006) Climate-carbon cycle feedback analysis: Results from the C4MIP model intercomparison. *International Journal of Climatology* 19, 3337–3353.
8. IPCC (2007) Summary for policymakers. In: S Solomon, D Qin, M Manning, Z Chen, M Marquis, KB Averyt, M Tignor and HL Miller (eds) *Climate Change 2007: The Physical Science Basis. Contribution of Working Group I to the Fourth Assessment Report of the Intergovernmental Panel on Climate Change*. Cambridge University Press, Cambridge, United Kingdom, and New York, United States of America.
9. Herbland A and Voituriez B (1979) Hydrological structure analysis for estimating the primary production in the tropical Atlantic ocean. *Journal of Marine Research* 37, 87–101.
10. Mackey DJ, Blanchot J, Higgins HW and Neveux J (2002) Phytoplankton abundances and community structure in the equatorial Pacific. *Deep-Sea Research II* 49, 2561–2582.
11. Dugdale RC, Wischmeyer AG, Wilkerson FP, Barber RT and others (2002) Meridional asymmetry of source nutrients to the equatorial Pacific upwelling ecosystem and its potential impact on ocean-atmosphere CO<sub>2</sub> flux; a data and modelling approach. *Deep-Sea Research II* 49, 2513–2531.
12. Landry MR and Kirchman DL (2002) Microbial community structure and variability in the tropical Pacific. *Deep-Sea Research II* 49, 2669–2693.
13. Zehr JP, Waterbury JB, Turner PJ, Montoya JP and others (2001) Unicellular cyanobacteria fix N<sub>2</sub> in the subtropical North Pacific Ocean. *Nature* 412, 635–638.
14. Dore JE, Letelier RM, Church MJ, Lukas R and Karl D (2008) Summer phytoplankton blooms in the oligotrophic North Pacific Subtropical Gyre: Historical perspective and recent observations. *Progress in Oceanography* 76, 2–38.
15. Karl D, Michaels A, Bergman B, Capone DG and others (2002) Dinitrogen fixation in the world's oceans. *Biogeochemistry* 57/58, 47–98.
16. Landry MR, Al-Mutairi H, Selph KE, Christensen S and Nunnery S (2001) Seasonal patterns of mesozooplankton abundance and biomass at Station ALOHA. *Deep-Sea Research II* 48, 2037–2061.

17. O'Neil JM and Roman MR (1994) Ingestion of the cyanobacterium *Trichodesmium* spp. by pelagic harpacticoid copepods *Macrosetella*, *Miracia* and *Oculosetella*. *Hydrobiologia* 292/293, 235–240.
18. Azam F, Fenchel T, Gray JG, Meyer-Reil LA and Thingstad T (1983) The ecological role of water-column microbes in the sea. *Marine Ecology Progress Series* 10, 257–263.
19. Sherr E and Sherr B (2008) Understanding roles of microbes in marine pelagic food webs: A brief history. In: DL Kirchman (ed) *Microbial Ecology of the Oceans*. John Wiley and Sons Inc., Hoboken, New Jersey, United States of America, pp. 27–44.
20. Richardson TL and Jackson GA (2007) Small phytoplankton and carbon export from the surface ocean. *Science* 315, 838–840.
21. Roger C (1994) Relationships among yellowfin and skipjack tuna, their prey-fish and plankton in the tropical western Indian Ocean. *Fisheries Oceanography* 3, 133–141.
22. Legand M, Bourret P, Fourmanoir P, Grandperrin R and others (1972) Relations trophiques et distributions verticales en milieu pélagique dans l'océan Pacifique intertropical. *Cahiers ORSTOM, Série Océanographie* 10, 303–393.
23. Potier M, Marsac F, Lucas V, Sabatié R and others (2004) Feeding partitioning among tuna taken in surface and mid-water layers: The case of yellowfin (*Thunnus albacares*) and bigeye (*T. obesus*) in the Western Tropical Indian Ocean. *Western Indian Ocean Journal Marine Science* 3, 51–62.
24. Young JW, Lansdell M, Riddoch S and Revill A (2006) Feeding ecology of broadbill swordfish, *Xiphias gladius* (Linnaeus, 1758), off eastern Australia in relation to physical and environmental variables. *Bulletin of Marine Science* 79, 793–811.
25. Graham BS, Grubbs D, Holland K and Popp BN (2007) A rapid ontogenic shift in the diet of juvenile yellowfin tuna from Hawaii. *Marine Biology* 150, 647–658.
26. Ménard F, Lorrain A, Potier M and Marsac F (2007) Isotopic evidence of distinct feeding ecologies and movement patterns in two migratory predators (yellowfin tuna and swordfish) of the western Indian Ocean. *Marine Biology* 153, 141–52.
27. Landsell M and Young JW (2007) Pelagic cephalopods from eastern Australia: Species composition, horizontal and vertical distribution determined from the diets of pelagic fishes. *Reviews in Fish Biology and Fisheries* 17, 125–138.
28. Young JW, Lansdell M, Hobday A, Dambacher J and others (2009) *Determining Ecosystem Effects of Longline Fishing in the Eastern Tuna and Billfish Fishery*. Final Report 2004/063, Fisheries Research and Development Corporation, Canberra, Australia.
29. Revill AT, Young JW and Lansdell M (2009) Stable isotopic evidence for trophic groupings and bioregionalization of predators and their prey in oceanic waters off eastern Australia. *Marine Biology* 156, 1241–1253.
30. Le Borgne R, Barber RT, Delcroix T, Inoue HY and others (2002) Pacific warm pool and divergence: Temporal and zonal variations on the equator and their effects on the biological pump. *Deep-Sea Research II* 49, 2471–2512.
31. Mackey DJ, O'Sullivan JE and Watson RJ (2002) Iron in the western Pacific: A riverine or hydrothermal source for iron in the Equatorial Undercurrent. *Deep-Sea Research I* 49, 877–893.
32. Murtugudde RG, Signorini SR, Christian JR, Busalacchi AJ and others (1999) Ocean color variability of the tropical Indo – Pacific basin observed by SeaWiFS during 1997–1998. *Journal of Geophysical Research* 104, 18,351–18,366.

33. Rodier M, Eldin G and Le Borgne R (2000) The western boundary of the equatorial Pacific upwelling: Some consequences of climatic variability on hydrological and planktonic properties. *Journal of Oceanography* 56, 463–471.
34. McClain CR, Christian JR, Signorini SR, Lewis MR and others (2002) Satellite ocean color observations of the tropical Pacific Ocean. *Deep-Sea Research II* 49, 2533–2560.
35. Ishii M, Saito S, Tokieda T, Kawano T and others (2004) Variability of surface layer CO<sub>2</sub> parameters in the western and central equatorial Pacific. In: M Shiyomi, H Kawahata, H Koizumi, A Tsuda and Y Awaya (eds) *Global Environmental Change in the Ocean and on Land*. Terra Pub, Tokyo, Japan, pp. 59–94.
36. Allain V, Kerandel J-A, Andrefouet S, Magron F and others (2008) Enhanced seamount location database for the western and central Pacific ocean: Screening and cross-checking of 20 existing datasets. *Deep-Sea Research I* 55, 1035–1047.
37. Le Bouteiller A, Leynaert A, Le Borgne R, Neveux J and others (2003) Changes of total and new primary production with nutrient in the equatorial Pacific (180°) during an ENSO cold event. *Journal of Geophysical Research* 108, 8136, doi:10.1029/2001JC000914
38. Brown SL, Landry MR, Neveux J and Dupouy C (2003) Microbial community abundance and biomass along a 180° transect in the equatorial Pacific during an ENSO cold phase. *Journal of Geophysical Research* 108, 8139, doi:10.1029/2001JC000817
39. Gorsky G, Le Borgne R, Picheral M and Stemmann L (2003) Marine snow latitudinal distribution in the equatorial Pacific along 180°. *Journal of Geophysical Research* 108, 8146, doi:10.1029/2001JC001064
40. Turk D, Lewis MR, Harrison WG, Kawano T and Asanuma I (2001) Geographical distribution of new production in the western/central equatorial Pacific during El Niño and non El Niño conditions. *Journal of Geophysical Research* 106, 4501–4515.
41. Mackey DJ, Parslow JS, Griffiths FB, Higgins HW and Tilbrook B (1997) Phytoplankton productivity and the carbon cycle in the western equatorial Pacific under ENSO and non-ENSO conditions. *Deep-Sea Research II* 44, 1951–1978.
42. Polovina JJ, Howell EA and Abecassis M (2008) Ocean's least productive waters are expanding. *Geophysical Research Letters* 35, L03618, doi:10.1029/2007GL031745
43. Ras J, Claustre H and Uitz J (2008) Spatial variability of phytoplankton pigment distributions in the subtropical South Pacific Ocean: Comparison between *in situ* and predicted data. *Biogeosciences* 5, 353–369.
44. Karl D (1999) A sea of change: Biogeochemical variability in the North Pacific Subtropical Gyre. *Ecosystems* 2, 181–214.
45. Dandonneau Y and Gohin F (1984) Meridional and seasonal variations of the sea surface chlorophyll concentration in the southwestern tropical Pacific (14 to 32°S, 160 to 175°E). *Deep-Sea Research* 31, 1377–1393.
46. Hayward TL (1987) The nutrient distribution and primary production in the central North Pacific. *Deep-Sea Research* 34, 1593–1627.
47. Barnett MA (1983) Species structure and temporal stability of mesopelagic fish assemblages in the Central gyres of the north and south Pacific Ocean. *Marine Biology* 74, 245–256.
48. Doty MS and Oguri M (1956) The island mass effect. *Journal du Conseil International pour l'Exploration de la mer* XXII, 33–37.
49. Gilmartin M and Revelante N (1974) The 'island mass effect' on the phytoplankton and primary production of the Hawaiian islands. *Journal of Experimental Marine Biology and Ecology* 16, 181–204.

50. Le Borgne R, Dandonneau Y and Lemasson L (1985) The problem of the island mass effect on chlorophyll and zooplankton standing crops around Mare (Loyalty islands) and new Caledonia. *Bulletin of Marine Science* 37, 450–459.
51. Roger C (1986) Macroplankton et micronekton dans le Pacifique tropical sud-ouest. *Océanographie Tropicale* 21, 153–165.
52. Matson EA (1993) Nutrient flux through soils and aquifers to the coastal zone of Guam (Mariana Islands). *Limnology and Oceanography* 38, 361–371.
53. Dupouy C (1990) La chlorophylle de surface observée par le satellite NIMBUS-7 dans une zone d'archipel (Nouvelle-Calédonie et Vanuatu). Une première analyse. *Bulletin Institut Océanographie Monaco* 6, 125–148.
54. Benitez-Nelson CR and McGillicuddy Jr DJ (2008) Mesoscale physical-biological linkages in the open ocean: An introduction to the results of the E-Flux and EDDIES programs. *Deep-Sea Research II* 55, 1133–1138.
55. Landry MR, Brown SL, Rii YM, Selph KE and others (2008) Depth-stratified phytoplankton dynamics in Cyclone Opal: A subtropical mesoscale eddy. *Deep-Sea Research II* 55, 1348–1359.
56. Landry MR, Decima M, Simmons MP, Hannides CCS and Daniels E (2008) Mesozooplankton biomass and grazing responses to Cyclone Opal: A subtropical mesoscale eddy. *Deep-Sea Research II* 55, 1378–1388.
57. Hénin C and Cresswell GR (2005) Upwelling along the western barrier reef of New Caledonia. *Marine and Freshwater Research* 56, 1005–1010.
58. Ganachaud A, Vega A, Rodier M, Dupouy C and others (2010) Observed impact of upwelling on water properties and biological activity off the Southwest coast of New Caledonia. *Marine Pollution Bulletin* 61, 449–464.
59. Owens WB and Hogg NG (1980) Oceanic observations of stratified Taylor columns near a bump. *Deep-Sea Research* 27, 1029–1045.
60. Roden GI (1987) Effects of seamounts and seamount chains on ocean circulation and thermohaline structure. In: BII Keating, P Friger, R Batiza and GW Boehlert (eds) *Seamounts, Islands and Atolls*. Geophysical Monograph 43, Washington, United States of America, pp. 335–354.
61. Genin A and Boehlert GW (1985) Dynamics of temperature and chlorophyll structures above a seamount: An oceanic experiment. *Journal of Marine Research* 43, 907–924.
62. Wilson CD and Boehlert GW (1990) *Acoustic Measurement of Micronekton Distribution over Southeast Hancock Seamount, Central Pacific Ocean*. National Oceanic and Atmospheric Administration publications CR/1990/9069, pp. 222–229.
63. De Forest L and Drazen J (2009) The influence of Hawaiian seamount on mesopelagic micronekton. *Deep-Sea Research I* 56, 232–250.
64. Kamykowski D (1974) Possible interactions between phytoplankton and semidiurnal internal tides. *Journal of Marine Research* 32, 67–89.
65. Lobel PS and Robinson AR (1986) The transport and entrapment of fish larvae by ocean mesoscale eddies and currents in Hawaiian waters. *Deep-sea Research Part A Oceanographic Research Papers* 33, 483–500.
66. Bertrand A, Bard F-X and Josse E (2002) Tuna food habits related to the micronekton distribution in French Polynesia. *Marine Biology* 140, 1023–1037.
67. Reid SB, Hirota J, Young RE and Hallacher LE (1991) Mesopelagic-boundary community in Hawaii: Micronekton at the interface between neritic and oceanic systems. *Marine Biology* 109, 427–440.

68. Benoit-Bird KJ and Au WWL (2006) Extreme diel horizontal migrations by a tropical nearshore resident micronekton community. *Marine Ecology Progress Series* 319, 1–14.
69. Bertrand A, Le Borgne R and Josse E (1999) Acoustic characterization of micronekton distribution in French Polynesia. *Marine Ecology Progress Series* 191, 127–140.
70. Hidaka K, Kawaguchi K, Tanabe T, Takahashi M and Kubodera T (2003) Biomass and taxonomic composition of micronekton in the western tropical-subtropical Pacific. *Fisheries Oceanography* 12, 112–125.
71. Moutin T, Van den Broeck N, Beker B, Dupouy C and others (2005) Phosphate availability controls *Trichodesmium* spp. biomass in the SW Pacific Ocean. *Marine Ecology Progress Series* 297, 15–21.
72. Landry MR, Ondrusek ME, Tanner SJ, Brown SL and others (2000) The biological response to iron fertilisation in the eastern equatorial Pacific (IronExII). I. Microplankton community abundances and biomass. *Marine Ecology Progress Series* 201, 27–42.
73. Landry MR, Constantinou J, Latasa M, Brown SL and others (2000) The biological response to iron fertilisation in the eastern equatorial Pacific (IronExII). III. Dynamics of phytoplankton growth and microzooplankton grazing. *Marine Ecology Progress Series* 201, 57–72.
74. Rollwagen Bollens GC and Landry MR (2000) Biological response to iron fertilisation in the eastern equatorial Pacific (IronEx II). II. Mesozooplankton abundance, biomass, depth distribution and grazing. *Marine Ecology Progress Series* 201, 43–56.
75. IRD (undated) [www.ird.nc/BIOGEOCHIMIE](http://www.ird.nc/BIOGEOCHIMIE) (accessed June 2010)
76. Wishner KFC, Ashijan CJ, Gelfman C, Gowing MM and others (1995) Pelagic and benthic ecology of the lower interface of the eastern tropical Pacific oxygen minimum zone. *Deep-Sea Research I* 42, 93–115.
77. Hutchins D (2008) Ocean acidification or CO<sub>2</sub> fertilisation? *Ocean Carbon Biogeochemistry News* 1, 1–4.
78. Brewer PG and Peltzer ET (2009) Limits to marine life. *Science* 324, 347–348.
79. Fabry VJ, Seibel BA, Feely RA and Orr JC (2008) Impacts of ocean acidification on marine fauna and ecosystem processes. *ICES Journal of Marine Science* 65, 414–432.
80. Gregg WW and Conkright ME (2002) Decadal changes in global ocean chlorophyll. *Geophysical Research Letters* 29, 1730, doi:10.1029/2002GL014689
81. Piontkovski SA and Castellani C (2007) Decline of zooplankton biomass in the tropical Atlantic Ocean. *Fourth International Zooplankton Production Symposium*, Book of Abstracts, Hiroshima, Japan.
82. Corno G, Karl D, Church MJ, Letelier RM and others (2007) Impact of climate forcing on ecosystem processes in the North Pacific Subtropical Gyre. *Journal of Geophysical Research* 112, doi:10.1029/2006JC003730
83. Sarmiento JL, Slater R, Barber R, Bopp L and others (2004) Response of ocean ecosystems to climate warming. *Global Biogeochemical Cycles* 18, doi:10.1029/2003GB002134
84. Aumont O, Maier-Reimer E, Blain S and Monfray P (2003) An ecosystem model of the global ocean including Fe, Si, P co-limitation. *Global Biogeochemical Cycles* 17, 1060, doi:10.1029/2001GB001745
85. Tagliabue A, Bopp L and Aumont O (2008) Ocean biogeochemistry exhibits contrasting responses to a large scale reduction in dust deposition. *Biogeosciences* 5, 11–24.

86. Langdon C, Takahashi T, Sweeney C, Chipman D and others (2000) Effect of calcium carbonate saturation state on the calcification rate of an experimental coral reef. *Global Biogeochemical Cycles* 14, 639–654.
87. Iglesias-Rodriguez M, Buitenhuis E and Raven J (2008) Response to comment on phytoplankton calcification in a high-CO<sub>2</sub> world peer reviewed article. *Science* 322, 1466.
88. Riebesell U, Bellerby R, Engel A, Fabry V and others (2008) Comment on 'Phytoplankton Calcification in a High-CO<sub>2</sub> World'. *Science* 322, 1466.
89. Iglesias-Rodriguez MD, Halloran PR, Rickaby REM, Hall IR and others (2008) Phytoplankton calcification in a high-CO<sub>2</sub> world. *Science* 320, 336–340.
90. Eppley RW (1972) Temperature and phytoplankton growth in the sea. *Fishery Bulletin US* 70, 1063–1085.
91. Furnas M and Crosbie ND (1999) *In situ* growth dynamics of the photosynthetic prokaryotic picoplankters *Synechococcus* and *Prochlorococcus*. *Bulletin de l'Institut Océanographique de Monaco* 19, 387–417.
92. Le Borgne R (1986) The release of soluble end products of metabolism. In: EDS Corner and SCM O'Hara (eds) *The Biological Chemistry of Marine Copepods*. Oxford University Press, New York, United States of America, pp. 109–164.
93. Vidal J (1980) Physioecology of zooplankton I – Effects of phytoplankton concentrations, temperature and body size on the net growth efficiency of *Calanus pacificus* and *Pseudocalanus* sp. *Marine Biology* 56, 203–212.
94. Arrieta JM, Weinbauer MG and Herndl GJ (2000) Interspecific variability in sensitivity of UV radiation and subsequent recovery in selected isolates of marine bacteria. *Applied and Environmental Microbiology* 66, 1468–1473.
95. Llabrés M and Agusti S (2006) Picophytoplankton cell death induced by UV radiation: Evidence for oceanic Atlantic communities. *Limnology and Oceanography* 51, 21–29.
96. Xue L, Zhong Y, Zhang T, An L and Wang X (2005) Effects of enhanced ultraviolet-B radiation on algae and cyanobacteria. *Critical Reviews in Microbiology* 31, 79–89.
97. McKinnon D, Richardson AJ, Burford MA and Furnas MJ (2007) Vulnerability of Great Barrier Reef plankton to climate change. In: JE Johnson and PA Marshall (eds) *Climate Change and the Great Barrier Reef: A Vulnerability Assessment*. 1<sup>st</sup> edition, Great Barrier Reef Marine Park Authority and Australian Greenhouse Office, Townsville, Australia, pp. 121–152.
98. Childress JJ and Seibel BA (1998) Life at stable low oxygen levels: Adaptations of animals to oceanic oxygen minimum layers. *The Journal of Experimental Biology* 201, 1223–1232.
99. Prince ED and Goodyear CP (2006) Hypoxia-based habitat compression of tropical pelagic fishes. *Fisheries Oceanography* 15, 451–464.
100. Parker-Stetter SL, Horne JK and Langness MM (2009) The influence of midwater hypoxia on nekton vertical migration. *ICES Journal of Marine Science* 66, 1296–1302.
101. Parker-Stetter SL and Horne JK (2009) Nekton distribution and midwater hypoxia: A seasonal, diel prey refuge? *Estuarine, Coastal and Shelf Science* 81, 13–18.
102. Orr JC, Fabry VJ, Aumont O, Bopp L and others (2005) Anthropogenic ocean acidification over the twenty-first century and its impact on calcifying organisms. *Nature* 437, 681–686.
103. Cohen AL and Holcomb M (2009) Why corals care about ocean acidification: Uncovering the mechanism. *Oceanography* 22, 118–127.

104. Ishizaka J, Harada K, Ishikawa K, Kiyosawa H and others (1997) Size and taxonomic plankton community structure and carbon flow at the equator, 175°E during 1990–1994. *Deep-Sea Research II* 44, 1927–1944.
105. Le Borgne R, Champalbert G and Gaudy R (2003) Mesozooplankton biomass and composition in the equatorial Pacific along 180. *Journal of Geophysical Research* 108, 8136, doi:10.1029/2000JC000745
106. Watson AJ and Orr JC (2003) Carbon dioxide fluxes in the global ocean. In: MJR Fasham (ed) *The Role of the Ocean Carbon Cycle in Global Change*. Springer Verlag, Berlin, Germany, pp. 123–143.
107. Brown CJ, Fulton EA, Hobday AJ, Matear RJ and others (2009) Effects of climate-driven primary production change on marine food webs: Implications for fisheries and conservation. *Global Change Biology* 16, 1194–1212.
108. Pauly D, Christensen V and Walters C (2000) Ecopath, Ecosim and Ecospace as tools for evaluating ecosystem impacts of fisheries. *ICES Journal of Marine Science* 57, 697–706.
109. Christensen V and Walters CJ (2004) Ecopath with Ecosim: Methods, capabilities and limitations. *Ecological Modelling* 172, 109–139.
110. Polovina JJ (1984) Model of a coral reef ecosystem 1. The Ecopath model and its application to French Frigate Shoals. *Coral Reefs* 3, 1–12.
111. Kitchell JF, Essington TE, Boggs CH, Schindler DE and Walters CJ (2002) The role of sharks and longline fisheries in a pelagic ecosystem of the Central Pacific. *Ecosystems* 5, 202–216.
112. Watters GM, Olson RJ, Francis RC, Fieldler PC and others (2003) Physical forcing and the dynamics of the pelagic ecosystem in the eastern tropical Pacific: Simulations with ENSO-scale and global-warming climate drivers. *Canadian Journal of Fisheries and Aquatic Sciences* 60, 1161–1175.
113. Griffiths SP, Fry GC, Kuhnert PM and Manson FJ (2009) Temporal and size-related variation in the diet, consumption rate, and daily ration of mackerel tuna (*Euthynnus affinis*) in neritic waters of eastern Australia. *ICES Journal of Marine Science* 66, 720–733.
114. Kloser RJ, Ryan T, Young J and Lewis M (2009) Acoustic observations of micronekton fish on the scale of an ocean basin: Potential and challenges. *ICES Journal of Marine Science* 66, 998–1006.
115. Lehodey P, Senina I and Murtugudde R (2008) A spatial ecosystem and populations dynamics model (SEAPODYM) – Modeling of tuna and tuna-like populations. *Progress in Oceanography* 78, 304–318.
116. Kleiber P, Hinton MG and Uozumi Y (2003) Stock assessment of blue marlin (*Makaira nigricans*) in the Pacific using MULTIFAN-CL. *Marine and Freshwater Research* 54, 349–360.
117. Langley A, Molony B, Bromhead D, Yokawa K and Wise B (2006) *Stock Assessment of Striped Marlin (Tetrapturus audax) in the Southwest Pacific Ocean*. Western and Central Pacific Fisheries Commission, Scientific Committee second regular session, 7–18 August 2006, Manila, Philippines, Document WCPFC-SC2-2006/SA-WP-6.
118. Hoyle S, Langley A and Hampton J (2008) *Stock Assessment of Albacore Tuna in the South Pacific Ocean*. Western and Central Pacific Fisheries Commission, 11–22 August 2008, Port Moresby, Papua New Guinea, Document WCPFC-SC4-2008/SA-WP-8.
119. Langley A, Hampton J, Kleiber P and Hoyle S (2008) *Stock Assessment of Bigeye Tuna in the Western and Central Pacific Ocean, Including an Analysis of Management Options*. Western and Central Pacific Fisheries Commission, 11–22 August 2008, Port Moresby, Papua New Guinea, Document WCPFC-SC4-2008/SA-WP-1.

120. Griffiths SP, Young JW, Landsell MJ, Campbell RA and others (2010) Ecological effects of longline fishing and climate change on pelagic ecosystem off Australia. *Reviews in Fish Biology and Fisheries* 20, 239–272.
121. Grandperrin R (1975) *Structures Trophiques Aboutissant aux Thons de Longue Ligne dans le Pacifique Sud-Ouest Tropical*. Thèse d'état de l'Université d'Aix-Marseille II, France.
122. Bertrand A, Josse E, Bach P and Dagorn L (2003) Acoustics for ecosystem research: Lessons and perspectives from a scientific programme focusing on tuna-environment relationships. *Aquatic Living Resources* 16, 197–203.
123. Hansell DA, Carlson CA, Bates NR and Poisson A (1997) Horizontal and vertical removal of organic carbon in the equatorial Pacific Ocean: A mass balance assessment. *Deep-Sea Research II* 9/10, 2115–2130.
124. Vinogradov ME (1981) Ecosystems of equatorial upwellings. In: AR Longhurst (ed) *Analysis of Marine Ecosystems*. Academic Press, London, United Kingdom, pp. 69–93.
125. Buesseler KO, Doney SC, Karl DM, Boyd PW and others (2008) Ocean fertilisation – Moving forward in a sea of uncertainty. *Science* 319, 162.
126. Eldin G and Rodier M (2003) Ocean physics and nutrients fields along 180° during an El Niño-Southern Oscillation cold phase. *Journal of Geophysical Research* 108, 8136, doi:10.1029/2000JC000746
127. Roman MR, Dam HG, Gauzens AL, Urban-Rich J and others (1995) Zooplankton variability on the equator at 140°W during the JGOFS EqPac study. *Deep-Sea Research II* 42, 673–693.
128. Le Borgne R and Rodier M (1997) Net zooplankton and the biological pump: A comparison between the oligotrophic and mesotrophic equatorial Pacific. *Deep-Sea Research II* 44, 2003–2023.
129. Le Borgne R and Landry MR (2003) EBENE: A JGOFS investigation of plankton variability and trophic interactions in the equatorial Pacific (180°). *Journal of Geophysical Research* 108, 8136, doi:10.1029/2001JC001252
130. Decima M, Landry MR and Rykaczewski R (2010) Broad-scale patterns in mesozooplankton biomass and grazing in the eastern equatorial Pacific. *Deep-Sea Research II* 58, 387–399.
131. Dussart BH (1965) Les différentes catégories de plancton. *Hydrobiologia* 26, 72–74.
132. UNESCO (1968) *Zooplankton Sampling*. Monographs on Oceanographic Methodology 2, UNESCO, Paris, France.

